



Published in final edited form as:

*Mol Pharm.* 2016 January 4; 13(1): 8–24. doi:10.1021/acs.molpharmaceut.5b00626.

## Molecular Imaging of Pancreatic Cancer with Antibodies

Christopher G. England<sup>1</sup>, Reinier Hernandez<sup>1</sup>, Savo Bou Zein Eddine<sup>1</sup>, and Weibo Cai<sup>1,2,3,\*</sup>

<sup>1</sup>Dept. of Medical Physics, University of Wisconsin – Madison, USA

<sup>2</sup>Dept. of Radiology, University of Wisconsin – Madison, USA

<sup>3</sup>University of Wisconsin Carbone Cancer Center, Madison, WI, USA

### Abstract

Development of novel imaging probes for cancer diagnostics remains critical for early detection of disease, yet most imaging agents are hindered by suboptimal tumor accumulation. To overcome these limitations, researchers have adapted antibodies for imaging purposes. As cancerous malignancies express atypical patterns of cell surface proteins in comparison to non-cancerous tissues, novel antibody-based imaging agents can be constructed to target individual cancer cells or surrounding vasculature. Using molecular imaging techniques, these agents may be utilized for detection of malignancies and monitoring of therapeutic response. Currently, there are several imaging modalities commonly employed for molecular imaging. These imaging modalities include positron emission tomography (PET), single-photon emission computed tomography (SPECT), magnetic resonance (MR) imaging, optical imaging (fluorescence and bioluminescence), and photoacoustic (PA) imaging. While antibody-based imaging agents may be employed for a broad range of diseases, this review focuses on the molecular imaging of pancreatic cancer, as there are limited resources for imaging and treatment of pancreatic malignancies. Additionally, pancreatic cancer remains the most lethal cancer with an overall 5-year survival rate of approximately 7%, despite significant advances in the imaging and treatment of many other cancers. In this review, we discuss recent advances in molecular imaging of pancreatic cancer using antibody-based imaging agents. This task is accomplished by summarizing the current progress in each type of molecular imaging modality described above. Also, several considerations for designing and synthesizing novel antibody-based imaging agents are discussed. Lastly, the future directions of antibody-based imaging agents are discussed, emphasizing the potential applications for personalized medicine.

### Keywords

Molecular imaging; pancreatic cancer; positron emission tomography (PET); single-photon emission computed tomography (SPECT); magnetic resonance imaging (MRI); optical imaging; photoacoustic tomography (PAT); antibodies

---

\*Corresponding author: Weibo Cai, Departments of Radiology and Medical Physics, University of Wisconsin–Madison, Room 7137, 1111 Highland Avenue, Madison, WI, 53705-2275, USA. Tel.: 608-262-1749; Fax: +1 608-265-0614; wcai@uwhealth.org.

**Conflicts of Interests:** The authors declare that they have no conflict of interest.

## 1. INTRODUCTION

Despite significant advances in early detection and treatment of many malignancies, pancreatic cancer remains the most lethal form of cancer with an overall 5-year survival rate of approximately 7%.<sup>1</sup> This dismal survival rate is attributed to several factors, including the lack of effective treatment regimens and inefficient screening technologies for detecting the disease during early stages. However, the overall 5-year survival rate is significantly improved (26%) for patients diagnosed during initial disease stages, when the primary tumor is localized with no metastatic lesions.<sup>1</sup> In addition to inefficient screening techniques, treatment of pancreatic cancer remains elusive as these highly heterogeneous and aggressive tumors swiftly develop resistance to available chemotherapeutics and radiation therapy.<sup>2</sup> While surgical resection offers the best survival rate and only potential cure, only 15–20% of patients are candidates for surgical intervention at the time of diagnosis.<sup>2</sup> For patients presenting with advanced stage disease, treatment options are limited to chemotherapy and radiation therapy, both minimally effective.

In 2015, an estimated 48,960 patients will be diagnosed with pancreatic cancer in the United States, along with 40,560 attributed deaths.<sup>1</sup> For comparison, pancreatic cancer is the fourth leading cause of cancer-related death worldwide, yet the Pancreatic Cancer Action Network<sup>®</sup> predicts that pancreatic malignancies will become the second leading cause of cancer-related death by 2020.<sup>3</sup> Most patients are asymptomatic during initial disease stages, attributing to the high percentage of patients diagnosed with advanced disease.<sup>4</sup> Currently, there is active research in discovering novel methods for enhancing the early detection of pancreatic malignancies, yet no reliable tools exist at this time. Screening of high-risk patients (e.g., cigarette smokers, family history of pancreatic cancer, personal history of chronic pancreatitis) could potentially lower the number of late diagnoses, yet high cost and limited known risk factors have hindered this approach.<sup>5, 6</sup> The purpose of this review article is to examine the recent advancements in molecular imaging of pancreatic cancer for early disease detection and therapeutic monitoring with antibody-based imaging agents.

## 2. ANTIBODIES FOR CANCER IMAGING

Effective imaging techniques facilitate early detection of malignancies and allow for non-invasive monitoring of therapeutic response in real time. Both early detection and therapeutic surveillance are essential for improving patient survival. Thus, there is a dire need for novel imaging contrast agents in the clinic. Researchers have applied several strategies for the development of new imaging agents, effectively targeting tumor tissue using small proteins, peptides, viruses, antibodies, among other targeting entities.<sup>7</sup> Historically, the first radiolabeled-antibody utilized for cancer imaging was approved by the FDA in 1993 for imaging of prostate cancer.<sup>8</sup>

Highly specific imaging contrast agents are required for non-invasive visualization of biomolecular processes through molecular imaging. Traditionally, *ex vivo* and *in vitro* techniques have been utilized for assessing protein expression, yet molecular imaging can provide similar details without requiring animal euthanasia or complex cell-based studies.<sup>9</sup> While researchers have designed hundreds of imaging contrast agents for both cancer

Author Manuscript

diagnostics and therapeutic surveillance, many of these novel probes are limited by suboptimal tumor accumulation.<sup>10</sup> Antibodies are employed to improve upon these limitations as molecular imaging probes. There are several properties that make antibodies suitable molecular imaging probe candidates, including their high specificity for specific antigens, potentially low immunogenicity, and high clinical relevance. Currently, there are several FDA-approved therapeutic antibodies for cancer treatment, and several other antibody-based treatments are seeking approval.<sup>11</sup> Also, antibodies are less likely to cause the off-target toxicity often associated with common chemotherapeutics, due to their high specificity for the protein of interest.<sup>12</sup>

Author Manuscript

While full antibodies are commonly adapted as molecular imaging probes, many studies have noted long blood circulation times and slow tumor accumulation as limiting factors in their potential clinical application.<sup>13</sup> The serum half-life of different immunoglobulin isotypes ranges from 2.5 days for IgE to 23 days for IgG in humans.<sup>14</sup> For this reason, construction of imaging probes using smaller antibody fragments (e.g., Fab', scFv and F(ab')<sub>2</sub>) has become common practice (Table 1). In addition, combinations of smaller antibody fragments have been constructed for optimized pharmacokinetic profiles. These include diabodies (divalent sc(Fv)<sub>2</sub> or trivalent [sc(Fv)<sub>2</sub>]<sub>2</sub>), minibodies that consists of two scFv fragments genetically linked to a C<sub>H</sub>3 domain, and triabodies created through genetically linking two scFv to an Fc fragment.<sup>15, 16</sup> Antibody fragments often display enhanced pharmacokinetics profiles in comparison to full antibodies, attributed to their shortened serum half-life and faster tumor accumulation.<sup>17</sup> A previous study using a murine antibody clearly displayed the different pharmacokinetic profiles of antibody fragments and full antibodies.<sup>17</sup> It was shown that Fab (0.2 days) cleared circulation faster than F(ab')<sub>2</sub> (0.5 days), which were both significantly faster than the whole antibody (8.5 days). In humans, whole antibodies display circulation times ranging from days to weeks, resulting in optimal tumor accumulation between 2–5 days post-injection.<sup>18</sup> While whole antibodies normally result in higher tumor accumulation as compared to fragmented antibodies, the time frame is not optimal for clinical purposes, as nuclear imaging would require multiple patient visits. In general, fragmented antibodies display shorter blood circulation times with maximum tumor accumulation normally occurring between 2 to 24 hr.<sup>18, 19</sup> Lastly, several researchers have investigated methods for improving the pharmacokinetics of antibody-based imaging agents, including the development of recombinant bispecific antibody fusion molecules. These imaging agents contain an antibody fragment fused to a protein (e.g., albumin) or two antibody fragments chemically-conjugated together. These antibody constructs can display prolonged circulation times *in vivo*, increased accumulation in tumor tissue, and potentially decrease immunogenicity.<sup>20</sup>

Author Manuscript

Several factors regarding the type of antibody (i.e. monoclonal, polyclonal, bispecific) and antibody class (i.e. IgG<sub>1</sub>, IgG<sub>2</sub>) should be considered before designing an antibody-based imaging agent. Monoclonal antibodies are more commonly employed as molecular imaging agent as they are highly monospecific, recognizing a single epitope of an antigen. In comparison, polyclonal antibodies are more rapidly produced, yet lack the purity levels obtained with monoclonal antibodies. Also, polyclonal antibodies do not meet the regulatory guidelines set forth for human use.<sup>21</sup> Several other molecular constructs of antibodies are

used to enhance the pharmacokinetic properties of the antibodies *in vivo*, including bispecific antibodies, tetrabodies, and diabodies.<sup>22</sup> Also, the class of antibody can alter its biodistribution and metabolism *in vivo*.

Several characteristics must be considered when designing novel antibody-based imaging agents. First, the antibody should be human monoclonal or humanized to reduce possible immunogenicity. This is accomplished through the transfer of complementarity-determining region residues from the donor mouse antibody to the human antibody template.<sup>23</sup> The binding properties of humanized antibodies are determined through affinity measurements, competitive binding assays, and biosensor analysis methods. Antibodies that fail to meet the required binding properties are modified or eliminated, while antibodies that display unaltered binding properties are examined for their biological activity.<sup>23</sup> Secondly, the antibody should display optimal kinetic profiles for targeting and clearance. This may be achieved by using fragmented antibodies or through enhanced neonatal Fc receptor (FcRn) binding.<sup>24</sup> Also, the antibody should remain highly stable in serum. Antibody stability is often modified through stability engineering of constant or variable domains and the addition of charged fusion tags.<sup>25</sup> Lastly, the antibody should be bivalent to assist in tissue targeting and retention, if possible.<sup>26, 27</sup> While the characteristics listed above specifically apply to antibody-based imaging agents, there are several general considerations applicable to designing any molecular imaging probe. Some features of optimized molecular imaging probes include rapid clearance from the blood to reduce background signal, high tissue permeability, increased selectivity and specificity for targeted tissues, fast clearance from non-targeted tissues, high reproducibility for clinical purposes, and simple pharmacokinetic profiles to allow for quantitative modeling.<sup>28</sup>

In addition to antibodies, there are several other classes of ligands commonly employed for targeting cancer. Some examples include viruses, peptides, low molecular weight proteins, and nanoparticles.<sup>29</sup> For example, several cytokines have been investigated as potential imaging agents, as they are small and undergo rapid clearance from circulation.<sup>29</sup> Also, peptides and aptamers are commonly employed as targeting ligands for imaging agents, yet glomerular transit and proteolysis often limit their use in preclinical applications.<sup>30</sup> Most other targeting ligands are constrained by lower binding affinity and specificity, in comparison to antibodies. Lastly, antibody-based imaging agents offer another advantage, as they can be used to help deliver cytotoxic radionuclides to malignancies.<sup>31</sup>

Currently, there are over 35 antibody-based treatment options approved for use in various cancer types, with a growth market around 20–30 billion dollars each year.<sup>32–34</sup> The safety profiles of these antibodies have been evaluated at pharmacological doses by the Food and Drug Administration (FDA). For this reason, FDA-approved antibodies are expected to function as suitable imaging agents, as doses required for molecular imaging are much lower than therapeutic doses.

### 3. MOLECULAR IMAGING OF PANCREATIC CANCER

Molecular imaging is the non-invasive examination of the cellular function and monitoring of molecular processes *in vivo* using specialized imaging agents. Nuclear medicine evolved

during the late 1950s with a predominant shift from anatomical imaging, using plain films and scintigraphy, to functional and hybrid imaging modalities.<sup>35</sup> For molecular imaging, specific molecular pathways are targeted for visualization using molecular imaging contrast agents. This allows for the non-invasive characterization and monitoring of disease progression, investigation of cellular processes occurring in real-time, assessment of drug/receptor interactions, and evaluation of the biodistribution of various compounds.<sup>36</sup> Also, molecular imaging may lessen the burden of identifying patients that may benefit from specific antibody treatment regimens, as invasive biopsies are currently used to identify patients.

Molecular imaging requires the use of specialized imaging contrast agents with enhanced targeting capabilities to ensure optimal tissue contrast. There are two key components of molecular imaging constructs, including a contrast agent for visualization and a tissue-specific ligand for actively targeting the tumor or diseased tissue of interest (Fig. 1).<sup>37</sup> The composition of contrast agents vary based upon the imaging modality, yet some common examples include positron-emitting isotopes, fluorescent dyes, and various nanoparticle platforms.<sup>9</sup> In most situations, these imaging agents are targeted to cell surface receptors upregulated in the disease of interest. In this review, we discuss the molecular imaging of pancreatic malignancies with antibody-based imaging constructs (e.g., radiolabeled antibodies, antibody-targeted nanoparticles, fluorescent-labeled antibodies).

There are several targets currently being explored for targeting of pancreatic cancer. For example, mesothelin is a membrane glycoprotein expressed in more than 90% of pancreatic cancers.<sup>38</sup> Also, cholecystokinin, gastrin, and progastrin have also been shown to be expressed in more than 90% of pancreatic cancers. PD-L1 is another target recently explored for imaging purposes, as it is highly expressed in pancreatic tumor cells and the microenvironment.<sup>39</sup> Some imaging agents have been targeted to signaling pathways in the epithelial layer of pancreatic cancer, including the epidermal growth factor receptor (EGFR) and insulin-like growth factor 1 receptor (IGF1R).<sup>38</sup> Targeting to the tumor stroma has also been accomplished through vascular endothelial growth factor (VEGFR), cyclooxygenase-2 (COX-2), matrix metalloproteinases (MMPs), and hedgehog signaling (through the tumor suppressor patched and oncogenic protein smoothened).<sup>38</sup> Other potential targets previously investigated in pancreatic cancer include urokinase-type plasminogen activator receptor (uPAR), Plectin-1, and MUC1.<sup>38, 40</sup> Several of these targets and others will be discussed in more detail later in this section. For more information regarding potential biological targets in pancreatic cancer, readers are directed to more detailed reviews on this topic.<sup>38, 41</sup>

Imaging of pancreatic cancer is crucial for improving patient survival, as most patients are diagnosed after the disease has metastasized to other organs. While antibody-based imaging agents may enhance early detection, their use in identifying patients more likely to respond to certain therapeutics and monitoring treatment response will significantly enhance the current survival rate. Molecular imaging utilizes specialized instrumentation for the diagnosis and therapeutic monitoring of disease progression including PET, single photon emission computed tomography (SPECT), MRI, optical imaging (e.g., bioluminescence and fluorescence), and photoacoustic (PA) imaging (Fig. 2).<sup>42</sup> While this review focuses on

detection of pancreatic malignancies, these versatile imaging modalities are commonly utilized for detection of most solid tumors and other diseases.

### 3.1 PET imaging of pancreatic cancer

In PET imaging, the administered contrast agent is radiolabeled with an isotope that decays by positron emission. PET detection is based on the coincidence detection of two antiparallel 511 keV gamma photons resulting from the positron-electron annihilation in tissue. A tomographic reconstruction of all detected lines of response is then performed to obtain an image of the three-dimensional distribution of the tracer.<sup>43</sup> PET imaging provides high sensitivity and excellent tissue penetration, which allows for quantitative detection of PET tracers in the picomolar range.<sup>44</sup> Several positron-emitting isotopes have been evaluated as potential radiosynthons for imaging pancreatic malignancies, including <sup>15</sup>O, <sup>11</sup>C, <sup>18</sup>F, <sup>61</sup>Cu, <sup>64</sup>Cu, and <sup>89</sup>Zr.<sup>45–48</sup> PET tracers are typically generated through covalent attachment of the isotope to an electrophilic group present in the biological molecule of interest, or via coordination with a suitable chelator.

Targeting of cell surface receptors upregulated in cancer remains the most promising strategy for designing molecular imaging probes. For example, Wang *et al.* constructed an antibody targeting the cell surface protein, known as GRP78.<sup>49</sup> Overexpression of GRP78 is linked to increased tumor growth, rapid drug resistance, and the development of highly metastatic disease. While GRP78 is overexpressed in most pancreatic cancers, it is expressed at low levels in normal pancreatic tissue and precancerous pancreatic lesions.<sup>50</sup> The novel antibody (MAb159) was conjugated to <sup>64</sup>Cu using the chelator 1,4,7,10-Tetraazacyclododecane-1,4,7,10-tetraacetic acid (DOTA).<sup>48</sup> MAb159 was raised against the glucose-related immunoglobulin heavy-chain binding protein (GRP78) and used for specific targeting of GRP78-expressing BxPC-3 pancreatic subcutaneous xenograft tumors. Peak intratumoral accumulation of  $18.3 \pm 1.0$  %ID/g was obtained at 48 hr post-injection (Fig. 3), as shown by PET imaging (Fig. 3A) and biodistribution (Fig. 3B). For comparison, non-targeted radiolabeled-human IgG was injected as control and displayed a tumor accumulation of only  $7.5 \pm 0.7$  %ID/g (Fig. 3C). Similar upregulated proteins have been investigated as potential targets for PET imaging of therapeutic response. For example, mesothelin is a small glycoprotein highly expressed in the majority of pancreatic adenocarcinomas, yet not expressed in most precancerous lesions. Kobayashi *et al.* developed an anti-mesothelin antibody (11-25) as a novel agent for PET imaging of subcutaneous xenograft tumor-bearing mice with three pancreatic cancer cell lines (BxPC-3<sup>high</sup>, CFPAC-1<sup>medium</sup>, and PANC-1<sup>low</sup>), with varying levels of mesothelin expression.<sup>51</sup> The mAb 11-25 was produced in hybridoma cells previously generated by immunizing mice with a recombinant mesothelin protein. Cell binding assays showed that DOTA-11-25 mAb and the native antibody displayed similar antigen reactivity and PET imaging revealed that <sup>64</sup>Cu-DOTA-11-25 mAb accumulated higher in mesothelin-expressing BxPC-3 and CFPAC-1 subcutaneous xenograft tumors.

<sup>89</sup>Zr is a relatively new radionuclide that has been employed for PET imaging of multiple cancers, as the isotope has become widely accessible during the last decade with several available chelating agents.<sup>52</sup> This unique isotope was utilized by Sugyo *et al.* to image the

transferrin receptor in transferrin-positive tumor-bearing mice using the monoclonal antibody TSP-A01.<sup>46</sup> The antibody was radiolabeled with <sup>89</sup>Zr, using p-isothiocyanatobenzyl-desferrioxamine (DFO) as the chelator, and the biodistribution and specificity were determined by PET. The transferrin receptor-positive tumor subcutaneous xenograft tumor model (MiaPaCa-2) was accurately identified using the <sup>89</sup>Zr-labeled antibody with a peak uptake of  $12.5 \pm 2.3$  %ID/g obtained at two days post-injection. This study demonstrated the potential use of this imaging probe for selecting patients that may benefit from anti-transferrin therapy. In addition, Sugyo *et al.* employed <sup>89</sup>Zr for imaging of CD147-expressing pancreatic tumors in tumor-bearing mice using an antibody targeting CD147 called 059-053.<sup>53</sup> CD147, also called EMMPRIN, is an immunoglobulin transmembrane protein highly expressed in malignant pancreatic cancer and expressed at low levels in precancerous lesions and pancreatitis.<sup>54</sup> It is involved in lymphocyte activation, induction of monocarboxylate transporters, and induction of several metalloproteinases (MMPs).<sup>55</sup> The antibody 059-053 was obtained from a large-scale human antibody library constructed using phage-display and was shown to inhibit the proliferation of pancreatic cancer cells.<sup>53</sup> MiaPaCa-2 subcutaneous xenograft tumors, shown to highly express CD147, displayed an uptake of  $11.0 \pm 1.3$  %ID/g at 24 hr post-injection, with a peak uptake of  $16.9 \pm 13.2$  %ID/g occurring six days post-injection. Also, an orthotopic mouse model of MiaPaCa-2 was established and displayed an uptake of 8.6 %ID/g at six days post-injection.

Antibodies are widely employed for the treatment of several other types of cancer and diseases.<sup>56–59</sup> These FDA-approved antibodies are excellent candidates for molecular imaging as they may be used for concurrent treatment and imaging of disease. For example, Boyle *et al.* examined the potential utilization of panitumumab, an FDA-approved human anti-EGFR antibody, for imaging of patient-derived pancreatic cancer xenograft and orthotopic tumors.<sup>60</sup> Pancreatic cancer, precancerous lesions, and chronic pancreatitis often overexpress EGFR, making it a suitable marker for early disease detection and therapeutic monitoring.<sup>61</sup> To accomplish this task, F(ab')<sub>2</sub> fragments of panitumumab were produced through proteolytic digestion, before labeling with <sup>64</sup>Cu. At 48 hr post-injection, tumor uptake values of <sup>64</sup>Cu-NOTA-panitumumab-F(ab')<sub>2</sub> were  $12.0 \pm 0.9$  %ID/g and  $11.8 \pm 0.9$  %ID/g in xenograft and orthotopic tumor models, respectively.

In another study, Viola-Villegas *et al.* modified an antibody targeting the tumor-associated cancer antigen 19-9 (CA19.9), known as 5B1.<sup>62</sup> The antibody 5B1 was previously generated and characterized from blood lymphocytes of patients immunized with the sLE<sup>a</sup>-KLH vaccine. In this study, 5B1 was radiolabeled with <sup>89</sup>Zr using DFO as the chelator and evaluated for the detection and staging of pancreatic cancer.<sup>63</sup> PET imaging revealed that <sup>89</sup>Zr-5B1 displayed significantly higher uptake in orthotopically implanted BxPC-3 tumors in comparison to <sup>18</sup>F-FDG, with tumor uptake values of  $30.7 \pm 6.6$  %ID/g and  $4.8 \pm 1.3$  %ID/g, respectively at 48 hr post-injection.<sup>62</sup> Also, a diabody of anti-CA19.9 was engineered by Girgis *et al.* from the variable regions of the monoclonal murine antibody 116-NS-19-9 using the NS116.19.9 hybridoma cell line.<sup>64</sup> The diabody was radiolabeled with <sup>124</sup>I and tumor uptake was compared between pancreatic subcutaneous xenograft tumors expressing low (MiaPaCa-2 in right shoulder) and high levels (Capan-2 or BxPC-3

in left shoulder) of CA19.9. Since the long serum half-life of full antibodies can potentially hinder the contrast between tumor and blood pools, this study employed a smaller antibody fragment (~55 kDa). The diabody displayed enhanced tumor accumulation with positive-to-negative tumor ratios of 11:1 and 6:1 for BxPC-2 and Capan-2 tumors at 20 hr post-injection, respectively. Also, there was five-fold more radioactivity in the tumor as compared to blood, which was adequate contrast for delineation between tumor tissue and background. While CA19.9 is overexpressed in pancreatic cancer and some precursor pancreatic lesions, overexpression in non-neoplastic conditions, ranging from benign obstructive jaundice to chronic pancreatitis, has limited its use as a diagnostic imaging marker.<sup>65</sup>

Hong *et al.* utilized the upregulation of tissue factor in pancreatic cancer as a potential target for molecular imaging.<sup>66</sup> Tissue factor is a transmembrane glycoprotein that activates the clotting cascade in non-diseased states, yet is known to cause thrombosis, tumor growth, and angiogenesis in cancerous tissue.<sup>67</sup> Tissue factor can be targeted for early detection of pancreatic lesions and monitoring of therapeutic response as it is highly expressed in precancerous pancreatic lesions, including 77% of pancreatic intraepithelial neoplasias (PanINs).<sup>68</sup> Targeting of tissue factor was accomplished using ALT-836, a chimeric monoclonal antibody developed by Altor BioSciences, which is currently in human clinical trials (NCT01325558). In BxPC-3-derived subcutaneous xenograft tumor-bearing mice, tumor accumulation of <sup>64</sup>Cu-NOTA-ALT-836 reached a peak of  $16.5 \pm 2.6$  %ID/g at 48 hr post-injection. As stated by the authors, this was the first utilization of molecular imaging for visualizing tissue factor expression *in vivo*.

Carcinocinoembryonic antigen-related cell adhesion molecule 6 (CEACAM-6) is a cell surface glycoprotein known to be highly expressed in most cancers, thus researchers have adapted this antibody as a potential imaging agent for therapeutic monitoring.<sup>69, 70</sup> Several studies have demonstrated strong correlations between high CEACAM-6 expression and increased rates of tumor metastasis and drug resistance.<sup>71, 72</sup> Recently, Niu *et al.* exploited the overexpression of CEACAM-6 for molecular imaging of BxPC-3-derived subcutaneous xenograft tumors by employing a full-length, heavy chain, and single domain antibody radiolabeled with <sup>64</sup>Cu-DOTA.<sup>73</sup> The heavy chain portion of the antibody was shown to be far superior to both the whole antibody and single domain antibody for imaging purposes, with higher tumor uptake and lower liver uptake of the contrast agent. Similarly, the scFv-Fc fragment of an antibody targeting (carcinoembryonic antigen) CEA was investigated by Girgis *et al.* as a potential PET imaging agent, since high expression of CEA was found in 84% of human pancreatic cancer specimens.<sup>74</sup> The fragmented antibody displayed a significantly decreased serum half-life in comparison to the full antibody at 27 hr and ten days, respectively. Also, a tumor/blood ratio of 4.0 was achieved, which is comparable to clinical studies and allowed for the clear delineation of tumor boundaries.

### 3.2 SPECT imaging of pancreatic cancer

While PET imaging relies upon the detection of positron-emitting isotopes, SPECT imaging detects single gamma radiation using an array of gamma cameras.<sup>75</sup> Several 2-D projections of the patient are acquired at multiple angles and later reconstructed using tomographic



reconstruction algorithms to form a 3-D image of radiotracer biodistribution.<sup>76</sup> While PET/CT imaging technologies in general offer superior resolution and quantitative capabilities, SPECT/CT technologies are more accessible in the clinic at a lower cost for patients.<sup>77</sup> Also, there is a wider range of approved radiotracers for SPECT imaging in comparison to PET imaging. Some common gamma emitters employed for SPECT imaging include <sup>99m</sup>Tc, <sup>111</sup>In, <sup>123</sup>I, and <sup>201</sup>Tl.<sup>78–80</sup> Availability of <sup>99</sup>Mo/<sup>99m</sup>Tc generators has significantly improved the accessibility of SPECT in limited access areas with no previous access to this imaging modality.<sup>81</sup> Incorporation of CT with SPECT or PET imaging modalities enhances disease detection by accounting for attenuation, resolution effects, and motion artifacts.<sup>82, 83</sup> Several studies have revealed synergistic improvements in disease detection and treatment monitoring with combined imaging modalities, as compared to single imaging techniques.<sup>84–86</sup> Currently, SPECT/CT is not commonly employed for detection of pancreatic malignancies in the clinic, yet improved imaging agents may promote its use in the future.

Recently, clinical imaging of mesothelin-expressing pancreatic cancer was monitored in six patients using an <sup>111</sup>In-labeled chimeric monoclonal antibody, known as amatuximab.<sup>87</sup> The antibody-based imaging probe, investigated in four patients with malignant mesothelioma and two patients with pancreatic adenocarcinoma, produced a tumor to background ratio 1.2, sufficient for distinguishing between tumor and normal tissue. Furthermore, this was the first clinical trial examining the safety and biodistribution of <sup>111</sup>In-amatuximab and the imaging tracer displayed a favorable dosimetry profile and was tolerated well in patients.

AXL receptor tyrosine kinase (RTK)-targeted antibodies were evaluated by Leconet *et al.* as a potential treatment option for pancreatic cancer.<sup>88, 89</sup> AXL RTK is linked to increased cellular proliferation and invasion of many cancers. Since AXL RTK is highly expressed in 76% of pancreatic adenocarcinoma patient samples, development of novel antibody-based therapies targeting this receptor could significantly advance the treatment of pancreatic malignancies. The inhibitory effects of these novel antibodies were evaluated using SPECT/CT imaging with <sup>125</sup>I-labeled antibody in pancreatic subcutaneous and orthotopic xenograft mouse models. Tumor growth and migration were significantly hindered by the antibody *in vitro*, thus demonstrating that anti-human AXL antibodies could be used for simultaneous imaging and immunotherapy of pancreatic malignancies in the future.<sup>88</sup>

Ferritin is an iron storage protein targeted by Sabbah *et al.* for concurrent imaging and treatment of pancreatic tumors.<sup>90</sup> AMB8LK, an antibody targeting ferritin, was conjugated with <sup>111</sup>In for SPECT/CT imaging using either DOTA or DTPA, as the chelating agent. SPECT/CT imaging showed high uptake of <sup>111</sup>In-DTPA-AMB8LK in mice with CAPAN-1 subcutaneous xenograft tumors, with  $23.6 \pm 3.9$  %ID/g at 72 hr post-injection (Fig. 4). In comparison to <sup>111</sup>In-DTPA-AMB8LK, <sup>111</sup>In-DOTA-AMB8LK accumulation peaked at 48 hours post-injection with  $12.6 \pm 3.9$  %ID/g (Fig. 4).<sup>90</sup> While it was shown *in vitro* that <sup>111</sup>In-DTPA-AMB8LK exhibited higher binding to ferritin and cells expressing the antigen, in comparison to <sup>111</sup>In-DOTA-AMB8LK, the authors did not provide a reason why the pharmacokinetics differed between DTPA- and DOTA-labeled AMB8LK. Sawada *et al.* further explored the use of <sup>111</sup>In for targeting pancreatic malignancies using a murine/human chimeric antibody.<sup>91</sup> Nd2 is a murine IgG1 antibody produced against the mucin fractions of

SW1990-derived xenograft tumors. Mucins function by limiting the activation of inflammatory responses, and mucin inhibitors have been shown to block the survival and tumorigenicity of human cancers in mouse models.<sup>92</sup> Several mucin proteins are overexpressed in pancreatic cancers and precancerous pancreatic lesions.<sup>93</sup> This study employed the mouse/human chimeric construct of Nd2, known as c-Nd2, to investigate its imaging and therapeutic potential in human pancreatic cancer. As expected, specific uptake of c-Nd2 was detected three days post-injection in 12 out of 14 patients, resulting in a sensitivity of 85.7%. Also, c-Nd2 displayed low immunogenicity with no cases of human anti-chimeric antibody (HACA) response in patients, which is known to alter the pharmacokinetic profile of antibodies.

In another study, claudin-4 was targeted by Foss *et al.* using an antibody conjugated with <sup>125</sup>I for SPECT/CT imaging, which displayed optimal tumor accumulation five days post-injection.<sup>94</sup> Claudin-4 is a membrane protein located in the tight junctions of cells and was shown to be overexpressed in most pancreatic cancers and many precancerous pancreatic lesions, making it a suitable biomarker for early disease detection.<sup>95, 96</sup> Similarly, an antibody was constructed to recognize and inhibit the adhesion of tumor cells to extracellular matrix proteins, with the overall purpose of inhibiting tumor growth.<sup>97, 98</sup> The <sup>111</sup>In-DOTA radiolabeled antibody (14C5), targeting  $\alpha_v\beta_5$  integrin, displayed a tumor uptake of  $35.84 \pm 8.64$  %ID/g at 48 hr post-injection while being investigated as a potential SPECT imaging agent in nude mice with Capan-1-derived subcutaneous xenograft tumors.<sup>98</sup>

Immunoscintigraphy is an imaging modality similar to SPECT, using a 2D planar gamma camera.<sup>99, 100</sup> While this technique was widely employed before the advent of SPECT, several studies have utilized immunoscintigraphy for imaging of pancreatic malignancies using antibody-based imaging agents. For example, an antibody targeting tumor-associated glycoprotein-72 (TAG-72), named B72.3, was radiolabeled with <sup>131</sup>I for detection of subcutaneous xenografts of human pancreatic carcinomas in nude mice.<sup>101</sup> While previous studies showed promising results, this study revealed the insufficient accumulation of the antibody-based probe in tumor tissue. However, a similar study successfully utilized a novel full and fragmented antibody (A7) labeled with <sup>125</sup>I and <sup>99m</sup>Tc for imaging of nude mice bearing human pancreatic cancer subcutaneous xenograft tumors.<sup>102, 103</sup> The ratio of radioactivity in tumor tissue, as compared to blood, was significantly higher than normal tissue, with the full antibody displaying higher tumor uptake as compared to the antibody fragment.

### 3.3 MR imaging of pancreatic cancer

Magnetic resonance imaging (MRI) relies on the ability of the magnetic dipoles of water protons to align under the influence of a strong magnetic field.<sup>104</sup> Briefly, when a strong magnetic field is applied, typically in the range of 1–7 Tesla, proton spins tend to adopt one two orientations, parallel or antiparallel with respect to the main magnetic field ( $B_0$ ). Given that parallel alignment is slightly energetically favored, a difference in population and energy between the two states is created. To produce an MR signal, the proton ensemble is perturbed from its equilibrium state through the use of radio-frequency excitation pulses. Upon termination of the excitation pulse, proton return to its original state by a process

called relaxation, in which energy is released as radiofrequency (RF) that can be detected by the MR scanner. Two main relaxation processes are observed in MR: longitudinal or spin-lattice relaxation that is characterized by a T1 time constant, and transversal or spin-spin relaxation, described by a T2 time constant. MR contrast arises from the difference in relaxation times T1 and T2 between various tissues. Additionally, contrast agents can manipulate the T1 and T2 times, effectively creating larger contrasts in T1-weighted or T2-weighted images. Readers are directed to detailed reviews for more detailed coverage of MR physical principles, image acquisition, and processing.<sup>104, 105</sup>

A significant advantage of MRI, in comparison to CT, is its superiority in soft tissue contrast and capability to provide additional details regarding tissue function, structure, and blood perfusion.<sup>106–108</sup> MRI is used for diagnosing pancreatic malignancies when confounding results are obtained from standard diagnostic techniques (e.g., ultrasound and multi-detector computed tomography).<sup>109</sup> While effective for imaging pancreatic cancer, the signal-to-noise ratio and presence of motion artifacts that arise from relatively slow acquisition times, should be improved. More effective targeting strategies that limit the off-target accumulation of imaging probes will enhance the sensitivity of MRI. Additionally, improved MR sequences using respiratory gating can palliate most motion artifacts.<sup>110</sup> The amount of contrast agent required for MRI is dependent upon the tumor model, as orthotopic xenograft models more closely resemble the biologic characteristics (e.g. hypovascular tumors) found in human malignancies. Engrafted models tend to underestimate the dose required for obtaining adequate MRI signal, as this hypervascularized model leads to increased intratumoral accumulation of injected agents. As an example, preclinical investigations of superparamagnetic iron oxides nanoparticles (SPIONs) for pancreatic cancer imaging have required doses ranging from approximately 2.5 g Fe/kg to more than 5 g Fe/kg.<sup>111, 112</sup>

While nanoparticles are commonly utilized in drug delivery, novel theranostic nanoparticles allow for concurrent imaging and treatment of disease.<sup>113</sup> For example, Deng *et al.* developed a multifunctional nanoimmunoliposomal platform for simultaneous loading of SPIONs and the anticancer agent, doxorubicin.<sup>111</sup> This novel theranostic nanoplatform was targeted to pancreatic malignancies using an anti-mesothelin antibody and imaging was evaluated in Panc-1-derived subcutaneous xenograft tumors. Targeted nanoparticles often displayed an enhanced transverse relaxivity that result in enhanced T2-weighted MR contrast. Wang *et al.* further explored the application of SPIONs for imaging pancreatic malignancies using an antibody targeting plectin-1.<sup>114</sup> Antibody-modified SPIONs showed highly specific uptake by Panc-1 cells expressing plectin-1 with excellent biocompatibility, serum stability, and high relaxivity *in vitro*.

Chemokine receptor 4 (CXCR4) plays a vital role in early embryonic development, yet expression in cancer cells facilitates the growth and spread of tumors.<sup>115, 116</sup> Additionally, CXCR4 expression was shown to be specific for pancreatic cancer tissue with minimal expression in normal pancreatic tissue.<sup>117</sup> He and colleagues modified ultrasmall SPIONs for MR imaging of pancreatic cancer using a monoclonal antibody specific for CXCR4.<sup>118</sup> The targeted probe CXCR4-SPIO displayed enhanced T2 ratio *in vitro*, allowing for semi-quantitative assessment of CXCR4 expression in four pancreatic cancer cell lines (AsPC-1,

BxPC-3, CFPAC-1, and Panc-1). As CXCR-4 is expressed in over 75% of human PanINs, this imaging probe could be used for early disease detection and therapeutic monitoring.<sup>119</sup>

In a similar study, Yang *et al.* examined the biodistribution and tumor uptake of iron oxide (IO) nanoparticles modified with an EGFR-targeted single-chain antibody (ScFvEGFR) in mice bearing EGFR-positive (MiaPaCa-2) orthotopic xenograft tumors (Fig. 5).<sup>120</sup> As EGFR is commonly overexpressed in most pancreatic malignancies and precursor lesions, EGFR-targeted probes could be used for both early disease detection and therapeutic monitoring.<sup>121</sup> The single-chain anti-EGFR antibody, consisting of the heavy and light chain variable domains linked by a small peptide, was only 20% the size of a normal antibody (25 kDa), yet the fragment maintained both high binding specificity and affinity for EGFR.<sup>120</sup> ScFvEGFR-IOs were synthesized by coating 10 nm IO nanoparticles with amphiphilic copolymers containing short poly(ethylene)-glycol (PEG) chains, before the addition of the fragmented antibody (Fig. 5A). ScFvEGFR-IO accumulation in tumor tissue resulted in enhanced MRI contrast at 5 hr and 30 hr post-injection, allowing for delineation of tumor boundaries (Fig. 5B). For comparison, non-targeted nanoparticles did not show any MRI signal decrease in the tumor after nanoparticle injection (Fig. 5B), thus proving that ScFvEGFR-IO uptake was dependent upon EGFR expression.

Magnevist<sup>®</sup> (gadopentetate dimeglumine), a commonly utilized paramagnetic imaging agents in cancer diagnostics to visualize lesions with abnormal vascularity, was employed by Pirolo *et al.* in the development of a novel theranostic liposomal nanoplatform for synchronized MRI and drug delivery.<sup>122</sup> Magnevist<sup>®</sup> was successfully loaded into liposomal complexes targeted with an anti-transferrin receptor single-chain antibody (TfRscFv). In Capan-1-derived orthotopic pancreatic tumor models, TfRscFv-targeted nanoparticles loaded with Magnevist showed both increased resolution and image intensity, as compared to freely circulating Magnevist<sup>®</sup>. In another report, Chen *et al.* targeted neutrophil gelatinase-associated lipocalin (NGAL) for imaging and therapy of pancreatic cancer by encapsulating gold nanoshells in silica epilayers doped with iron oxide and indocyanine green dye.<sup>123</sup> This novel platform, containing two imaging agents, displayed enhanced contrast for both optical imaging and T2-weighted MRI with higher tumor contrast in nude mice bearing AsPC-1-derived subcutaneous xenografts, as compared to non-targeted nanoparticles. As NGAL is expressed in malignant pancreatic cancers and early dysplastic lesions of the pancreas, newly developed NGAL-targeting imaging agents may be employed for both early disease detection and therapeutic monitoring.<sup>124</sup>

### 3.4 Optical (fluorescence and bioluminescence) imaging of pancreatic cancer

Optical imaging has grown significantly over the last decade as a more cost-efficient molecular imaging modality that utilizes the excitation properties of fluorophores.<sup>125</sup> Increased spatial resolution and real-time imaging are main advantages of optical imaging, in comparison to PET and SPECT imaging.<sup>126</sup> Also, optical imaging does not require administration of ionizing radiation to patients, which eliminates unnecessary radiation exposure and allows for multiple dose administrations. Instead, optical imaging utilizes the light properties of fluorescent or bioluminescent compounds for *in vivo* imaging. While effective for preclinical investigation of pancreatic malignancies, a major drawback for the

clinical application of optical imaging is the limited depth penetration into tissue.<sup>127, 128</sup> Contrast agents designed for optical imaging are within the wavelength range 650–1450 nm, commonly termed the optical imaging window.<sup>129</sup> An optical imaging window is a spectral region where light can penetrate tissue more deeply, yet is not affected by the autofluorescence of water or other endogenous chromophores (e.g., hemoglobin, melanin) found between 200–650 nm.<sup>130</sup> Commonly utilized contrast agents for fluorescence imaging include near infrared (NIR) dyes, quantum dots, and gold nanoparticles.<sup>9</sup>

While identification of both primary and metastatic disease significantly impacts patient survival, current imaging modalities often fail to provide sufficient visualization of tumor margins. For this reason, pancreatic tumors are often incompletely resected during surgical procedures and many laparoscopies result in incorrect disease staging. To improve visualization of pancreatic malignancies during laparoscopies, many researchers have employed optical imaging agents for assisting surgeons in identifying tumor margins and potentially locating metastatic lesions. For this purpose, Cao and collaborators investigated an anti-CEA fluorophore-conjugated antibody for detection of both primary and metastatic BxPC-3-derived orthotopic pancreatic xenografts in nude mice using fluorescence laparoscopy (Fig. 6).<sup>131–133</sup> Tumors could be identified much faster using fluorescence laparoscopy (FL), as compared to traditional bright field laparoscopy (BFL) (Fig. 6A, B).<sup>131</sup> Also, the sensitivity of each platform for detecting metastatic lesions was compared, with FL displaying higher sensitivity in comparison to BFL at 96.3% and 40.4%, respectively. While larger tumors were easily detected by both FL and BFL, FL was superior in detecting metastatic disease or smaller tumors deeper in the tissue (Fig. 6C), as confirmed by *ex vivo* studies.<sup>131</sup>

In a similar study, Boonstra and colleagues exploited the overexpression of CEA, found in the majority of pancreatic cancers, for visualizing pancreatic tumors.<sup>134</sup> A novel CEA-targeted near-infrared fluorescent tracer was established by attaching a single-chain antibody fragment to 800CW. The single-chain variable fragment was constructed from the humanized version of MFE-23, the first single-chain antibody molecule to be used in clinical trials.<sup>135</sup> Single-chain antibody fragments were utilized in this study for their rapid blood clearance through the kidneys and uniform tumor penetration, which allowed for imaging at early time points with high tumor-to-background ratios.<sup>134</sup> They found a peak tumor-to-background ratio of  $5.1 \pm 0.6$  at 72 hr post-injection, noted to be suitable for discriminating tumor boundaries in mice bearing BxPC-3-derived orthotopic pancreatic xenografts. Similar investigators have described the potential use of CEA-targeting antibodies to improve fluorescence-guided surgical resection of pancreatic malignancies.<sup>136–141</sup>

Currently, the tumor marker CA19.9 is used to help differentiate between pancreatic malignancies and other diseases (e.g. pancreatitis), for assessing cancer progression, treatment efficacy, and monitoring cancer recurrence.<sup>142, 143</sup> Additionally, CA19.9 has been investigated as a potential target for molecular imaging. In one study, McElroy *et al.* developed an antibody targeting CA19.9 conjugated with a green fluorophore, for enhancing the intraoperative visualization of primary and metastatic pancreatic lesions in BxPC-3-derived orthotopic tumor models.<sup>144</sup> The fluorescent labeled antibody allowed for clear

visualization of the primary tumor at 24 hr post-injection. Additionally, small metastatic lesions within the spleen and liver were also visualized. In a similar study, Hiroshima *et al.* further evaluated the potential targeting of CA19.9 for imaging of patient-derived orthotopic xenografts during fluorescence-guided surgical procedures.<sup>145</sup>

While CA19.9 functions as a tumor marker found in patient serum, it suffers from low sensitivity and high false positives.<sup>146</sup> For these reasons, newer biomarkers are currently being investigated for pancreatic cancer. A potential candidate is MUC1, a membrane-bound glycoprotein expressed in over 90% of pancreatic cancers, commonly associated with increased lethality.<sup>147, 148</sup> Park *et al.* targeted MUC1 using a fluorescent antibody, by attaching the antibody CT2 to DyLight 550. The new imaging tracer was successfully employed for optical imaging of both BxPC-3-derived orthotopic and subcutaneous xenograft tumors in nude mice.<sup>149</sup> Previously, MUC1 was shown to be expressed at low levels in normal pancreatic tissues, high levels in primary and metastatic pancreatic ductal adenocarcinomas, and moderate to high levels in PanINs.<sup>93</sup> For this reason, MUC1-based imaging agents may be potentially utilized for early disease detection and therapeutic monitoring.

Also, quantum dots have been exploited as potential optical imaging agents for their high quantum yields, in combination with excellent biostability and photostability.<sup>150</sup> For example, Yong *et al.* constructed non-cadmium-based quantum dots modified with anti-claudin 4 for imaging of MiaPaCa-2 cells.<sup>151</sup> Non-cadmium based quantum dots have been shown to be less toxic than commonly utilized cadmium quantum dots, which release cadmium and selenium into the biological environment during degradation.<sup>152</sup> They evaluated the toxicity by incubating varying concentrations of indium phosphide (core)- zinc sulfide (shell), or InP/ZnS, quantum dots with MiaPaCa-2 cells and found the quantum dots to be non-toxic at high concentrations (i.e., 10 mg/mL and 100 mg/mL).<sup>151</sup>

In many instances, imaging agents are constructed for use with multiple imaging modalities. For example, Kobayashi *et al.* developed a multimodality contrast agent for PET and optical imaging using an antibody against mesothelin, co-functionalized with <sup>64</sup>Cu and Alexa Fluor® 750.<sup>51</sup> As expected, imaging revealed significant fluorescence signal in mesothelin-positive pancreatic subcutaneous xenograft tumors in BALB/c nu/nu mice (Panc-1, CFPAC-1, and BxPC-3), while those models with low mesothelin expression exhibited minimal fluorescence signal. In a similar study, EGFR was targeted by Kampmeier *et al.* with a single-chain antibody fragment of cetuximab, constructed using the SNAP-tag technology, and further functionalized for optical imaging with an NIR dye (BG-747).<sup>153</sup> Rapid and highly specific accumulation of the tracer was exhibited at 10 hr post-injection, with a tumor to background ratio of  $33.2 \pm 6.3$ . The fragmented antibody showed enhanced tumor uptake and faster clearance in comparison to the full-length antibody.

### 3.5 PA imaging of pancreatic cancer

Compared to other imaging modalities described in this review, PA imaging is considered to be relatively new, as it was first introduced for biomedical imaging purposes in 1981 by Theodore Bowen.<sup>154</sup> PA is based on the formation of acoustic pressure waves from electromagnetic energy. Simply, the patient's tissue is exposed to short laser pulses at

several wavelengths, resulting in the formation of ultrasound waves detected by an ultrasonic transducer.<sup>155, 156</sup> The rapid thermoelastic and thermal expansion of the tissue caused by the absorbance of laser photons causes the production of ultrasound waves.<sup>157</sup> Similar to optical imaging, exposure to ionizing x-ray radiation is not needed, making it possible to image patients multiple times with no health hazards. There are several advantages to PA imaging as it combines both optical and ultrasound imaging into a single instrument. Some of these benefits included high spatial resolution, high tissue contrast and enhanced spectroscopic-based specificity.<sup>158</sup> Recent advances in PA tomography have made whole-body small animal imaging feasible, allowing for real-time tracking of imaging agents *in vivo*.<sup>159</sup> PA imaging offers a unique capability in addition to imaging of non-endogenous imaging agents. There are several endogenous chromophores in biological tissue capable of produce PA signals, including hemoglobin, myoglobin, certain lipids, and melanin.<sup>160</sup> For this reason, it is possible to monitor many biological processes *in vivo*, including angiogenesis during tumor formation, development of intratumoral hypoxia, and visualization of blood flow within tissues.<sup>161, 162</sup> While endogenous chromophores make it possible to visualize tumor vasculature, non-endogenous imaging agents are needed for specifically targeting tumor cells or surrounding vasculature.

As a dual imaging modality, PA systems do not rely upon the ballistic photons required for optimal imaging. For this reason, it is possible to imaging tissue at greater penetration depths with high resolution.<sup>163</sup> Previous studies have demonstrated that penetration depths of 4–6 cm are feasible, with the use of highly efficacious contrast agents within an optimal wavelength range.<sup>164–166</sup> Similar to optical imaging, NIR wavelength range contrast agent allow for optimal tissue depth penetration, as tissue absorption is minimized in this wavelength range.<sup>167</sup> Examples of previously developed PA imaging agents include NIR dyes, carbon nanotubes, gold nanoparticles, SPIOs, methylene blue, and indocyanine green.<sup>159</sup> Since few studies have employed PA imaging for visualization of pancreatic malignancies; this section includes other targeting ligands besides antibodies. Recently, Lakshman and Needles described a methodology for screening and quantifying the tumor microenvironment of orthotopic pancreatic tumors using the Vevo<sup>®</sup> PA imaging system.<sup>168</sup> In this study, intratumoral perfusion was investigated using gas-filled microbubbles, with peripheral regions of the tumor showing high perfusion and core regions showing minimal perfusion.

In 2012, Homan *et al.* synthesized antibody-conjugated silver nanoplates using biocompatible chemical reagents (Fig. 7).<sup>169</sup> The nanoparticles displayed a maximum peak absorbance near 900 nm, making them optimal for PA imaging. The edge length and thickness of the silver nanoplates was shown to be  $128 \pm 25.9$  nm and  $18 \pm 2.7$  nm through transmission electron microscopy (TEM), respectively (Fig. 7A). An EGFR-targeted antibody was attached via the FC portion to the silver nanoplates, allowing for optimal targeting capabilities. Dark field microscopy confirmed the targeting efficiency and high specificity between the EGFR-nanoplates and pancreatic cancer cells (MPanc-96 and L3.6pl) *in vitro*. Cellular uptake of EGFR-targeted silver nanoplates was higher than uptake of polyethylene glycol (PEG)-modified nanoplates. However, this further confirmed the high specificity of the antibody-based platform for targeting EGFR (Fig. 7B). A

combination of ultrasonography and PA imaging was utilized to acquire images with laser pulses between 740 and 940 nm (Fig. 7C). Multiplex imaging of non-endogenous and endogenous contrast agents was accomplished, with EGFR-modified nanoplates depicted in yellow, oxygenated blood shown as red and deoxygenated blood illustrated as blue. Two-dimensional cross-sections and 3-D reconstructions were shown, proving that nanoplates selectively accumulated in the tumor and were easily differentiated from endogenous blood components (Fig. 7D). While it was visually determined that uptake of EGFR-targeted silver nanoplates was higher than uptake of polyethylene glycol (PEG)-modified nanoplates *in vivo*, these data were not quantified.

Several studies have successfully employed PA imaging for detecting and monitoring pancreatic malignancies using non-antibody based imaging agents. For example, Homan *et al.* developed a novel metallodielectric nanoplatform, by entrapping silica cores in silver cage nanoparticles, shown to enhance PA imaging contrasts in pancreatic tissues.<sup>170</sup> Also, protein-based PA imaging agents have been constructed for targeting EGFRb<sup>171</sup> and sigma-2 receptor<sup>172</sup> in pancreatic cancer. In the future, PA imaging may be employed for examining anti-cancer treatment response using theranostic nanoparticles, in combination with monitoring of the pharmacokinetic properties of diagnostic and therapeutic agents *in vivo*.

#### 4. CHALLENGES IN ANTIBODY TARGETING

Molecular imaging agents are constructed from a broad range of targeting entities. As discussed, the high specificity and small size of antibodies make them suitable imaging candidates, yet all imaging agents require optimization before utilization in animal studies. Several factors have been shown to influence the pharmacokinetics and targeting efficiency of antibodies for imaging purposes, including the molecular weight, Fc domains, valency, and specificity.<sup>13</sup> For example, the presence of Fc domains increases the circulation time of antibody-based imaging agents *in vivo*. While this provides more time for the imaging agent to interact with the target receptor, faster clearance leads to enhanced contrast and sensitivity for molecular imaging purposes. Also, antibodies may undergo binding and to non-targeted cells, decreasing the amount of imaging agent available for tumor binding.

The number of target antigens per cell and the rate of internalization are additional factors known to influence the pharmacokinetics of antibody-based imaging agents.<sup>8</sup> Additionally, the imaging agent dosage will need to be adjusted if the target protein is present at low concentrations in the blood, as this may decrease the blood circulation time of the imaging probe. Targeting of tumor cells remains difficult for most antibody-based imaging agents, as the harsh microenvironment of solid tumors may limit the access and binding imaging agents to tumor cells. Previous studies have shown that solid tumors display limited extravasation of molecules across the capillary walls, due to high interstitial fluid pressure.<sup>173</sup> Some researchers have attempted to bypass the need for extravasation by selectively targeting the tumor vasculature (e.g. CD105).<sup>174, 175</sup> Regions of highly heterogeneous pancreatic tumor tissue display various levels of hypoxia and necrosis, which may limit the access of imaging agents to portions of the tumor.<sup>176</sup> Also, the highly acidic



microenvironment may cause irreversible damage to antibody conformation and function, resulting in decreased binding affinity.

In addition to the pharmacokinetic challenges, the high production cost associated with producing monoclonal antibodies is another factor limiting the use of antibody-based imaging agents.<sup>177</sup> Companies developing antibodies for clinical applications are required to strictly adhere to several costly procedures and standards. Manufacturers must harvest the cell cultures needed for antibody production, before undergoing several steps to ensure the purification standards required for FDA-approval of monoclonal antibodies.<sup>13</sup> Currently, the retail price of therapeutic antibodies range from \$700 for bevacizumab (100mg) to \$1,700 for eculizumab.<sup>178</sup> While smaller quantities of the antibody are required for molecular imaging in comparison to therapy, manufacturers must consider the expensive production costs associated with radioisotope production and other requirements.

As pancreatic cancer is a highly heterogeneous and genetically complex disease, it is difficult to identify potential biomarker targets for molecular imaging of all pancreatic cancer patients.<sup>179</sup> Many of the biomarkers currently being investigated are expressed in a portion of pancreatic cancers, making them unsuitable for the entire population. For this reason, the discovery of biomarkers expressed in the majority of pancreatic cancers is critically needed. Also, visualization of pancreatic metastases requires increased presence of antigen on the surface of malignant cells, as compared to the primary tumor. Despite effective targeting strategies, antibodies may be hindered by the dense tumor stroma found in pancreatic tumors, consisting of increased amounts of stromal cells and extracellular matrix proteins. For more information regarding the biological barriers of pancreatic cancer, readers are directed to a detailed review.<sup>179</sup>

## 5. CLINICAL IMAGING OF PANCREATIC CANCER: CURRENT STRATEGIES

As molecular imaging is in the infant stages of development, clinical imaging of pancreatic cancer is dependent upon standardized procedures. Pancreatic cancer is detected using several clinical imaging techniques, often dependent on the expertise of the physician, instrument availability, and patient symptoms.<sup>4</sup> Currently, multi-sectional computed tomography (CT) is the most widely employed technique for assessing possible pancreatic disease, as this instrument offers high spatial resolution with moderately fast scan times.<sup>180</sup> Newer multislice helical computerized tomography (CT) scanners have displayed superior detection and staging accuracy of pancreatic cancer, as compared to traditional CT imaging, with detection accuracies of 90–95%.<sup>181</sup> The procedure for CT imaging of pancreatic cancer includes the use of oral water as a negative intraluminal contrast and intravenously injected iodinated contrast material.

Ultrasonography (US) examination is another imaging modality commonly utilized for diagnosing pancreatic cancer, yet this method lacks the sensitivity and reliability needed for staging the disease.<sup>182</sup> US is often the initial test used in symptomatic patients, as it remains inexpensive and highly accessible. For patients with jaundice or biliary ductal dilatation, endoscopic retrograde cholangiopancreatography (ERCP) may be performed to assess the

pancreas for tumors or other possible conditions.<sup>183</sup> Also, this technique may be used to biopsy the tumor and provide physicians information for determining treatment plans.

Endoscopic US (EUS) is another reliable imaging modality for detecting pancreatic cancer when performed by trained professionals.<sup>184</sup> Some studies have suggested that EUS may be as useful as CT imaging for detecting and staging pancreatic cancer, with an overall staging accuracy greater than 85%. This clinical imaging modality requires highly trained specialists and is not readily accessible worldwide. In combination with EUS, fine-needle aspiration (EUS-FNA) is useful for taking biopsies of abnormal pancreatic lesions.<sup>184</sup>

If these imaging modalities fail to provide consistent results, MRI or PET imaging is employed to confirm the diagnosis and stage of the disease. For MRI, patients receive an intravenous injection of gadolinium, as pancreatic cancer is hypointense on gadolinium-enhanced T1- weighted images. This is due to the hypovascularity and increased fibrous stroma found in pancreatic tumors.<sup>185</sup> In addition, diffusion-weighted MRI (DWI) was shown to accurately differentiate pancreatic cancer from pancreatitis in patients.<sup>186</sup> Due to the movement from breathing and bowel peristalsis, motion artifacts have limited the use of MRI for clinical imaging of pancreatic cancer. PET imaging using <sup>18</sup>F-FDG may be more sensitive for detecting early malignancies, as changes in tissue metabolism (i.e., glucose metabolism) usually predate any structural changes of the pancreas.<sup>187</sup> While newer dual modality PET-CT imaging systems are becoming widely available worldwide, the high cost associated with these instruments remains a limiting factor.

## 6. CONCLUSIONS AND FUTURE PERSPECTIVES

Recent advances in molecular imaging have altered the way we diagnose and monitor several diseases, including highly metastatic and drug-resistant pancreatic malignancies. While overall survival rates have improved for most cancers, pancreatic cancer remains the most lethal form of cancer in the United States. Despite significant research efforts, current treatment strategies remain limited and ineffective in most cases, resulting in a 5-year mortality rate of 93%.<sup>1</sup> This high mortality is attributed to both inefficient early detection strategies, coupled with ineffective first line treatments. To assist in the development of novel imaging therapeutic agents, researchers have evaluated several targeting entities as potential imaging agents, ranging from small molecular weight proteins to highly specific antibodies. Advances in molecular imaging of pancreatic cancer may provide imperative information regarding genotypic and phenotypic properties of the tumor and associated microenvironment. In return, this novel knowledge can be utilized for enhancing both cancer diagnoses and furthering our exploration of therapeutic monitoring in the future.

Extensive examination of molecular imaging has occurred during the last two decades, yet several challenges in the field remain unsolved.<sup>36</sup> The key limitation of molecular imaging is the development of exogenous imaging agents, as developing or discovering novel entities for receptor targeting can be both expensive and time-consuming. Since molecular imaging relies heavily upon active imaging agents, additional research into the development of novel molecular imaging agent is required. Another limitation is the current instrumentation, as both low spatial resolution and sensitivity can significantly hinder successful disease

monitoring, even with effective imaging agents. Also, current molecular imaging instrumentation is costly and unavailable to many academic and research facilities.<sup>188</sup> For molecular imaging to become standard practice, these modalities must be accessible by more researchers in the future. Lastly, clinical translation of these imaging modalities remains unclear and highly debatable, which may be resolved through added collaborative efforts from researchers in combination with standardization of imaging practices and multicenter clinical trials.<sup>189–191</sup>

In this review, five molecular imaging modalities were examined. When designing future research studies involving molecular imaging, the current limitations of each modality should be considered. A limiting factor of PET imaging is that it requires short-lived radioisotopes that must be created in costly cyclotrons.<sup>192, 193</sup> Also, radiation can produce harmful health hazards, yet minimization of these health risks are accomplished by limiting the patient exposure through lower doses of radioactivity. Lastly, PET imaging suffers from low spatial resolution, which limits our visualization of malignancies in some instances.<sup>194, 195</sup> For example, the invasion of adjacent structures of pancreatic tissue and vasculature may be unnoticeable with PET imaging, making it difficult for physicians to plan surgical procedures.<sup>196</sup> In comparison to PET, SPECT is limited by both lower resolution and less sensitivity.<sup>197</sup> About the strengths of PET and SPECT imaging, both modalities are not hindered by tissue depth and display high sensitivity.<sup>198, 199</sup>

MRI has several advantages including its unlimited depth penetration, high spatial resolution, excellent soft tissue contrast, and it does not require radioactive exposure.<sup>200</sup> While a useful imaging modality, MRI suffers from poor sensitivity and long acquisition times.<sup>201–203</sup> Next, optical imaging has become widely available in many research institutes in the last decade, yet the clinical translation remains uncertain at present. While optical imaging combines high sensitivity with no ionizing radiation requirement and low cost, this system is limited by low sensitivity and light attenuation at increased tissue depths.<sup>204</sup> As the multimodality instrument combining optical and ultrasound imaging, PA imaging can image at increased tissue depths up to 5 cm.<sup>205, 206</sup> Unlike optical imaging, the spatial resolution of PA imaging is not significantly affected by tissue depth.<sup>207</sup> In comparison to the limitless penetration of MRI, PET, and SPECT, the limited depth of penetration for PA imaging remains a critical hindrance to potential clinical translation.

In the future, both molecular imaging instrumentation and tracers will become more widely accessible for research purposes. As a pathway to personalized medicine, patients at risk for certain diseases may be screened using molecular imaging agents highly specific for certain disease models. For diseases with high mortality rates attributed to late symptom onset, early screening is predicted to save millions of lives. During the next decade, the field of molecular is expected to see significant growth, attributed to the development of improved imaging agents and instrumentation.

## Acknowledgments

This work was supported, in part, by the University of Wisconsin - Madison, the Department of Defense (W81XWH-11-1-0644), the National Institutes of Health (NIBIB/NCI 1R01CA169365, P30CA014520,

T32CA009206, and 5T32GM08349), the National Science Foundation (DGE-1256259), and the American Cancer Society (125246-RSG-13-099-01-CCE).

## References

1. Zhang Z, Liu S, Xiong H, Jing X, Xie Z, Chen X, Huang Y. Electrospun Pla/Mwcnts Composite Nanofibers for Combined Chemo- and Photothermal Therapy. *Acta Biomater.* 2015; 26:115–123. [PubMed: 26260417]
2. Long J, Zhang Y, Yu X, Yang J, LeBrun DG, Chen C, Yao Q, Li M. Overcoming Drug Resistance in Pancreatic Cancer. *Expert Opin Ther Targets.* 2011; 15:817–828. [PubMed: 21391891]
3. Rahib L, Smith BD, Aizenberg R, Rosenzweig AB, Fleshman JM, Matrisian LM. Projecting Cancer Incidence and Deaths to 2030: The Unexpected Burden of Thyroid, Liver, and Pancreas Cancers in the United States. *Cancer Res.* 2014; 74:2913–2921. [PubMed: 24840647]
4. Tempero MA, Arnoletti JP, Behrman S, Ben-Josef E, Benson AB, Berlin JD, Cameron JL, Casper ES, Cohen SJ, Duff M, Ellenhorn JDI, Hawkins WG, Hoffman JP, Kuvshinoff BW, Malafa MP, Muscarella P, Nakakura EK, Sasson AR, Thayer SP, Tyler DS, Warren RS, Whiting S, Willett C, Wolff RA. Pancreatic Adenocarcinoma: Clinical Practice Guidelines in Oncology. *J Natl Compr Cancer Netw.* 2010; 8:972–1017.
5. Maitra A, Hruban RH. Pancreatic Cancer. *Annu Rev Pathol.* 2008; 3:157–188. [PubMed: 18039136]
6. Bruenderman E, Martin RC 2nd. A Cost Analysis of a Pancreatic Cancer Screening Protocol in High-Risk Populations. *Am J Surg.* 2015; 210:409–416. [PubMed: 26003200]
7. Agdeppa ED, Spilker ME. A Review of Imaging Agent Development. *AAPS J.* 2009; 11:286–299. [PubMed: 19415506]
8. Olafsen T, Wu AM. Antibody Vectors for Imaging. *Semin Nucl Med.* 2010; 40:167–181. [PubMed: 20350626]
9. Hellebust A, Richards-Kortum R. Advances in Molecular Imaging: Targeted Optical Contrast Agents for Cancer Diagnostics. *Nanomedicine (Lond).* 2012; 7:429–445. [PubMed: 22385200]
10. Jiang L, Tu Y, Shi H, Cheng Z. Pet Probes Beyond (18)F-Fdg. *J Biomed Res.* 2014; 28:435–446. [PubMed: 25469112]
11. Scott AM, Wolchok JD, Old LJ. Antibody Therapy of Cancer. *Nat Rev Cancer.* 2012; 12:278–287. [PubMed: 22437872]
12. Lin MZ, Teitell MA, Schiller GJ. The Evolution of Antibodies into Versatile Tumor-Targeting. *Clin Cancer Res.* 2005; 11:129–138. [PubMed: 15671537]
13. Chames P, Van Regenmortel M, Weiss E, Baty D. Therapeutic Antibodies: Successes, Limitations and Hopes for the Future. *Br J Pharmacol.* 2009; 157:220–233. [PubMed: 19459844]
14. Lobo ED, Hansen RJ, Balthasar JP. Antibody Pharmacokinetics and Pharmacodynamics. *J Pharm Sci.* 2004; 93:2645–2668. [PubMed: 15389672]
15. Holliger P, Hudson PJ. Engineered Antibody Fragments and the Rise of Single Domains. *Nat Biotechnol.* 2005; 23:1126–1136. [PubMed: 16151406]
16. Todorovska A, Roovers RC, Dolezal O, Kortt AA, Hoogenboom HR, Hudson PJ. Design and Application of Diabodies, Triabodies and Tetrabodies for Cancer Targeting. *J Immunol Methods.* 2001; 248:47–66. [PubMed: 11223068]
17. Covell DG, Barbet J, Holton OD, Black CD, Parker RJ, Weinstein JN. Pharmacokinetics of Monoclonal Immunoglobulin G1, F(Ab')<sub>2</sub>, and Fab' in Mice. *Cancer Res.* 1986; 46:3969–3978. [PubMed: 3731067]
18. Thurber GM, Schmidt MM, Wittrup KD. Antibody Tumor Penetration: Transport Opposed by Systemic and Antigen-Mediated Clearance. *Advanced drug delivery reviews.* 2008; 60:1421–1434. [PubMed: 18541331]
19. Massuger LF, Claessens RA, Pak KY, Boerman OC, Daddona PE, Koenders EB, Kenemans P, Corstens FH. Tissue Distribution of 99mTc, 111In and 123I-Ov-T1 3 Fab' in Ovarian Carcinoma Bearing Nude Mice. *Int J Rad Appl Instrum B.* 1991; 18:77–83. [PubMed: 1707043]
20. Muller D, Karle A, Meissburger B, Hofig I, Stork R, Kontermann RE. Improved Pharmacokinetics of Recombinant Bispecific Antibody Molecules by Fusion to Human Serum Albumin. *J Biol Chem.* 2007; 282:12650–12660. [PubMed: 17347147]

21. Lipman NS, Jackson LR, Trudel LJ, Weis-Garcia F. Monoclonal Versus Polyclonal Antibodies: Distinguishing Characteristics, Applications, and Information Resources. *ILAR J.* 2005; 46:258–268. [PubMed: 15953833]
22. Goldenberg DM, Chatal JF, Barbet J, Boerman O, Sharkey RM. Cancer Imaging and Therapy with Bispecific Antibody Pretargeting. *Update Cancer Ther.* 2007; 2:19–31. [PubMed: 18311322]
23. Tsurushita N, Hinton PR, Kumar S. Design of Humanized Antibodies: From Anti-Tac to Zenapax. *Methods.* 2005; 36:69–83. [PubMed: 15848076]
24. Presta LG. Engineering of Therapeutic Antibodies to Minimize Immunogenicity and Optimize Function. *Advanced drug delivery reviews.* 2006; 58:640–656. [PubMed: 16904789]
25. Rouet R, Lowe D, Christ D. Stability Engineering of the Human Antibody Repertoire. *FEBS Lett.* 2014; 588:269–277. [PubMed: 24291820]
26. Wu AM. Engineered Antibodies for Molecular Imaging of Cancer. *Methods.* 2014; 65:139–147. [PubMed: 24091005]
27. Adams GP, Weiner LM. Monoclonal Antibody Therapy of Cancer. *Nat Biotechnol.* 2005; 23:1147–1157. [PubMed: 16151408]
28. Khalil MM, Tremoleda JL, Bayomy TB, Gsell W. Molecular Spect Imaging: An Overview. *Int J Mol Imaging.* 2011; 2011:796025. [PubMed: 21603240]
29. Chen K, Chen X. Design and Development of Molecular Imaging Probes. *Curr Top Med Chem.* 2010; 10:1227–1236. [PubMed: 20388106]
30. Wang AZ, Farokhzad OC. Current Progress of Aptamer-Based Molecular Imaging. *J Nucl Med.* 2014; 55:353–356. [PubMed: 24525205]
31. Mattes MJ. Radionuclide-Antibody Conjugates for Single-Cell Cytotoxicity. *Cancer.* 2002; 94:1215–1223. [PubMed: 11877748]
32. Lawrence S. Billion Dollar Babies-Biotech Drugs as Blockbusters. *Nat Biotech.* 2007; 25:380–382.
33. Huang ZQ, Buchsbaum DJ. Monoclonal Antibodies in the Treatment of Pancreatic Cancer. *Immunotherapy.* 2009; 1:223–229. [PubMed: 20046965]
34. Kalofonos HP, Grivas PD. Monoclonal Antibodies in the Management of Solid Tumors. *Curr Top Med Chem.* 2006; 6:1687–1705. [PubMed: 17017951]
35. Tian J, Cong W, Bai J, Jiang M, Liang W. Recent Advances in Molecular Imaging. *Int J Biomed Imaging.* 2007; 2007:73198. [PubMed: 18274656]
36. James ML, Gambhir SS. A Molecular Imaging Primer: Modalities, Imaging Agents, and Applications. *Physiol Rev.* 2012; 92:897–965. [PubMed: 22535898]
37. Chen ZY, Wang YX, Lin Y, Zhang JS, Yang F, Zhou QL, Liao YY. Advance of Molecular Imaging Technology and Targeted Imaging Agent in Imaging and Therapy. *Biomed Res Int.* 2014; 2014:819324. [PubMed: 24689058]
38. Cinar P, Tempero MA. Monoclonal Antibodies and Other Targeted Therapies for Pancreatic Cancer. *Cancer J.* 2012; 18:653–664. [PubMed: 23187854]
39. Heskamp S, Hobo W, Molkenboer-Kuenen JD, Olive D, Oyen WJ, Dolstra H, Boerman OC. Noninvasive Imaging of Tumor Pd-L1 Expression Using Radiolabeled Anti-Pd-L1 Antibodies. *Cancer Res.* 2015; 75:2928–2936. [PubMed: 25977331]
40. Konkalmatt PR, Deng D, Thomas S, Wu MT, Logsdon CD, French BA, Kelly KA. Plectin-1 Targeted Aav Vector for the Molecular Imaging of Pancreatic Cancer. *Front Oncol.* 2013; 3:84. [PubMed: 23616947]
41. Garrido-Laguna I, Hidalgo M. Pancreatic Cancer: From State-of-the-Art Treatments to Promising Novel Therapies. *Nat Rev Clin Oncol.* 2015; 12:319–334. [PubMed: 25824606]
42. Pichler BJ, Wehrl HF, Judenhofer MS. Latest Advances in Molecular Imaging Instrumentation. *J Nucl Med.* 2008; 49(Suppl 2):5S–23S. [PubMed: 18523063]
43. Gambhir SS. Molecular Imaging of Cancer with Positron Emission Tomography. *Nat Rev Cancer.* 2002; 2:683–693. [PubMed: 12209157]
44. Stockhofe K, Postema JM, Schieferstein H, Ross TL. Radiolabeling of Nanoparticles and Polymers for Pet Imaging. *Pharmaceuticals (Basel).* 2014; 7:392–418. [PubMed: 24699244]

45. Hubalewska-Dydejczyk A, Sowa-Staszczak A, Tomaszuk M, Stefanska A. Glp-1 and Exendin-4 for Imaging Endocrine Pancreas. A Review. Labeled Glucagon-Like Peptide-1 Analogues: Past, Present and Future. *Q J Nucl Med Mol Imaging*. 2015; 59:152–160. [PubMed: 25719487]
46. Sugyo A, Tsuji AB, Sudo H, Nagatsu K, Koizumi M, Ukai Y, Kurosawa G, Zhang MR, Kurosawa Y, Saga T. Preclinical Evaluation of (8)(9)Zr-Labeled Human Antitransferrin Receptor Monoclonal Antibody as a Pet Probe Using a Pancreatic Cancer Mouse Model. *Nucl Med Commun*. 2015; 36:286–294. [PubMed: 25460304]
47. Kubo S, Yamamoto K, Magata Y, Iwasaki Y, Tamaki N, Yonekura Y, Konishi J. Assessment of Pancreatic Blood Flow with Positron Emission Tomography and Oxygen-15 Water. *Ann Nucl Med*. 1991; 5:133–138. [PubMed: 1797067]
48. Zhao C, Chen Z, Ye X, Zhang Y, Zhan H, Aburano T, Tian M, Zhang H. Imaging a Pancreatic Carcinoma Xenograft Model with <sup>11</sup>c-Acetate: A Comparison Study with <sup>18</sup>f-Fdg. *Nucl Med Commun*. 2009; 30:971–977. [PubMed: 19696689]
49. Wang H, Li D, Liu S, Liu R, Yuan H, Krasnoperov V, Shan H, Conti PS, Gill PS, Li Z. Small-Animal Pet Imaging of Pancreatic Cancer Xenografts Using a <sup>64</sup>cu-Labeled Monoclonal Antibody, Mab159. *J Nucl Med*. 2015; 56:908–913. [PubMed: 25908833]
50. Zhe-Yu N, Qiao-Fei L, Meng-Yi W, Li Z, Lu-Tian Y, Quan L, Yu-Pei Z. Changes in the Expression of Glucose-Regulated Protein 78 in the Occurrence and Progression of Pancreatic Cancer in Mouse Models. *Zhongguo Yi Xue Ke Xue Yuan Xue Bao*. 2015; 37:259–263. [PubMed: 26149133]
51. Kobayashi K, Sasaki T, Takenaka F, Yakushiji H, Fujii Y, Kishi Y, Kita S, Shen L, Kumon H, Matsuura E. A Novel Pet Imaging Using (6)(4)Cu-Labeled Monoclonal Antibody against Mesothelin Commonly Expressed on Cancer Cells. *J Immunol Res*. 2015; 2015:268172. [PubMed: 25883990]
52. Zhang Y, Hong H, Cai W. Pet Tracers Based on Zirconium-89. *Curr Radiopharm*. 2011; 4:131–139. [PubMed: 22191652]
53. Sugyo A, Tsuji AB, Sudo H, Nagatsu K, Koizumi M, Ukai Y, Kurosawa G, Zhang MR, Kurosawa Y, Saga T. Evaluation of (89)Zr-Labeled Human Anti-Cd147 Monoclonal Antibody as a Positron Emission Tomography Probe in a Mouse Model of Pancreatic Cancer. *PLoS One*. 2013; 8:e61230. [PubMed: 23577210]
54. Zhang W, Erkan M, Abiatari I, Giese NA, Felix K, Kaye H, Buchler MW, Friess H, Kleeff J. Expression of Extracellular Matrix Metalloproteinase Inducer (Emmprin/Cd147) in Pancreatic Neoplasm and Pancreatic Stellate Cells. *Cancer Biol Ther*. 2007; 6:218–227. [PubMed: 17224648]
55. Xiong L, Edwards CK 3rd, Zhou L. The Biological Function and Clinical Utilization of Cd147 in Human Diseases: A Review of the Current Scientific Literature. *Int J Mol Sci*. 2014; 15:17411–17441. [PubMed: 25268615]
56. Chan CE, Chan AH, Hanson BJ, Ooi EE. The Use of Antibodies in the Treatment of Infectious Diseases. *Singapore Med J*. 2009; 50:663–672. quiz 673. [PubMed: 19644620]
57. Weiner LM, Surana R, Wang S. Monoclonal Antibodies: Versatile Platforms for Cancer Immunotherapy. *Nat Rev Immunol*. 2010; 10:317–327. [PubMed: 20414205]
58. Chan AC, Carter PJ. Therapeutic Antibodies for Autoimmunity and Inflammation. *Nat Rev Immunol*. 2010; 10:301–316. [PubMed: 20414204]
59. Beck A, Wurch T, Bailly C, Corvaia N. Strategies and Challenges for the Next Generation of Therapeutic Antibodies. *Nat Rev Immunol*. 2010; 10:345–352. [PubMed: 20414207]
60. Boyle AJ, Cao PJ, Hedley DW, Sidhu SS, Winnik MA, Reilly RM. MicroPET/Ct Imaging of Patient-Derived Pancreatic Cancer Xenografts Implanted Subcutaneously or Orthotopically in Nod-Scid Mice Using (64)Cu-Nota-Panitumumab F(Ab')<sub>2</sub> Fragments. *Nucl Med Biol*. 2015; 42:71–77. [PubMed: 25456837]
61. Ozaki N, Ohmuraya M, Ida S, Hashimoto D, Ikuta Y, Chikamoto A, Hirota M, Baba H. Serine Protease Inhibitor Kazal Type 1 and Epidermal Growth Factor Receptor Are Expressed in Pancreatic Tubular Adenocarcinoma, Intraductal Papillary Mucinous Neoplasm, and Pancreatic Intraepithelial Neoplasia. *J Hepatobiliary Pancreat Sci*. 2013; 20:620–627. [PubMed: 23475261]
62. Viola-Villegas NT, Rice SL, Carlin S, Wu X, Evans MJ, Sevak KK, Drobjnak M, Ragupathi G, Sawada R, Scholz WW, Livingston PO, Lewis JS. Applying Pet to Broaden the Diagnostic Utility

- of the Clinically Validated Ca19.9 Serum Biomarker for Oncology. *J Nucl Med.* 2013; 54:1876–1882. [PubMed: 24029655]
63. Sawada R, Sun SM, Wu X, Hong F, Ragupathi G, Livingston PO, Scholz WW. Human Monoclonal Antibodies to Sialyl-Lewis (Ca19.9) with Potent Cdc, Adcc, and Antitumor Activity. *Clin Cancer Res.* 2011; 17:1024–1032. [PubMed: 21343375]
64. Girgis MD, Kenanova V, Olafsen T, McCabe KE, Wu AM, Tomlinson JS. Anti-Ca19-9 Diabody as a Pet Imaging Probe for Pancreas Cancer. *J Surg Res.* 2011; 170:169–178. [PubMed: 21601881]
65. Shi C, Merchant N, Newsome G, Goldenberg DM, Gold DV. Differentiation of Pancreatic Ductal Adenocarcinoma from Chronic Pancreatitis by Pam4 Immunohistochemistry. *Arch Pathol Lab Med.* 2014; 138:220–228. [PubMed: 24476519]
66. Hong H, Zhang Y, Nayak TR, Engle JW, Wong HC, Liu B, Barnhart TE, Cai W. Immuno-Pet of Tissue Factor in Pancreatic Cancer. *J Nucl Med.* 2012; 53:1748–1754. [PubMed: 22988057]
67. Kasthuri RS, Taubman MB, Mackman N. Role of Tissue Factor in Cancer. *J Clin Oncol.* 2009; 27:4834–4838. [PubMed: 19738116]
68. Khorana AA, Ahrendt SA, Ryan CK, Francis CW, Hruban RH, Hu YC, Hostetter G, Harvey J, Taubman MB. Tissue Factor Expression, Angiogenesis, and Thrombosis in Pancreatic Cancer. *Clin Cancer Res.* 2007; 13:2870–2875. [PubMed: 17504985]
69. Scholzel S, Zimmermann W, Schwarzkopf G, Grunert F, Rogaczewski B, Thompson J. Carcinoembryonic Antigen Family Members Ceacam6 and Ceacam7 Are Differentially Expressed in Normal Tissues and Oppositely Deregulated in Hyperplastic Colorectal Polyps and Early Adenomas. *Am J Pathol.* 2000; 156:595–605. [PubMed: 10666389]
70. Blumenthal RD, Leon E, Hansen HJ, Goldenberg DM. Expression Patterns of Ceacam5 and Ceacam6 in Primary and Metastatic Cancers. *BMC Cancer.* 2007; 7:2. [PubMed: 17201906]
71. Duxbury MS, Ito H, Zinner MJ, Ashley SW, Whang EE. Ceacam6 Gene Silencing Impairs Anoikis Resistance and in Vivo Metastatic Ability of Pancreatic Adenocarcinoma Cells. *Oncogene.* 2004; 23:465–473. [PubMed: 14724575]
72. Duxbury MS, Ito H, Benoit E, Waseem T, Ashley SW, Whang EE. A Novel Role for Carcinoembryonic Antigen-Related Cell Adhesion Molecule 6 as a Determinant of Gemcitabine Chemoresistance in Pancreatic Adenocarcinoma Cells. *Cancer Res.* 2004; 64:3987–3993. [PubMed: 15173012]
73. Niu G, Murad YM, Gao H, Hu S, Guo N, Jacobson O, Nguyen TD, Zhang J, Chen X. Molecular Targeting of Ceacam6 Using Antibody Probes of Different Sizes. *J Control Release.* 2012; 161:18–24. [PubMed: 22568933]
74. Girgis MD, Olafsen T, Kenanova V, McCabe KE, Wu AM, Tomlinson JS. Targeting Cea in Pancreas Cancer Xenografts with a Mutated Scfv-Fc Antibody Fragment. *EJNMMI Res.* 2011; 1:24. [PubMed: 22214289]
75. de Jong M, Essers J, van Weerden WM. Imaging Preclinical Tumour Models: Improving Translational Power. *Nat Rev Cancer.* 2014; 14:481–493. [PubMed: 24943811]
76. DePuey EG. Advances in Spect Camera Software and Hardware: Currently Available and New on the Horizon. *J Nucl Cardiol.* 2012; 19:551–581. quiz 585. [PubMed: 22456968]
77. Hicks RJ, Hofman MS. Is There Still a Role for Spect-Ct in Oncology in the Pet-Ct Era? *Nat Rev Clin Oncol.* 2012; 9:712–720. [PubMed: 23149896]
78. Hnatowich DJ. Recent Developments in the Radiolabeling of Antibodies with Iodine, Indium, and Technetium. *Semin Nucl Med.* 1990; 20:80–91. [PubMed: 2404343]
79. Moffat FL Jr, Pinsky CM, Hammershaimb L, Petrelli NJ, Patt YZ, Whaley FS, Goldenberg DM. Clinical Utility of External Immunoscintigraphy with the Immu-4 Technetium-99m Fab' Antibody Fragment in Patients Undergoing Surgery for Carcinoma of the Colon and Rectum: Results of a Pivotal Phase Iii Trial. The Immunomedics Study Group. *J Clin Oncol.* 1996; 14:2295–2305. [PubMed: 8708720]
80. Ha L, Mansberg R, Nguyen D, Bui C. Increased Activity on in-111 Octreotide Imaging Due to Radiation Fibrosis. *Clin Nucl Med.* 2008; 33:46–48. [PubMed: 18097260]
81. Pillai MR, Dash A, Knapp FF Jr. Sustained Availability of 99mtc: Possible Paths Forward. *J Nucl Med.* 2013; 54:313–323. [PubMed: 23255729]

82. Chen CL, Wang Y, Lee JJ, Tsui BM. Toward Quantitative Small Animal Pinhole Spect: Assessment of Quantitation Accuracy Prior to Image Compensations. *Mol Imaging Biol.* 2009; 11:195–203. [PubMed: 19048346]
83. Hwang AB, Franc BL, Gullberg GT, Hasegawa BH. Assessment of the Sources of Error Affecting the Quantitative Accuracy of Spect Imaging in Small Animals. *Phys Med Biol.* 2008; 53:2233–2252. [PubMed: 18401059]
84. Von Schulthess GK, Hany TF. Imaging and Pet-Pet/Ct Imaging. *J Radiol.* 2008; 89:438–447. quiz 448. [PubMed: 18408643]
85. Lee JS, Kim JH. Recent Advances in Hybrid Molecular Imaging Systems. *Semin Musculoskeletal Radiol.* 2014; 18:103–122. [PubMed: 24715444]
86. Koba W, Jelicks LA, Fine EJ. Micropet/Spect/Ct Imaging of Small Animal Models of Disease. *Am J Pathol.* 2013; 182:319–324. [PubMed: 23219729]
87. Lindenberg L, Thomas A, Adler S, Mena E, Kurdziel K, Maltzman J, Wallin B, Hoffman K, Pastan I, Paik CH, Choyke P, Hassan R. Safety and Biodistribution of 111In-Amatuximab in Patients with Mesothelin Expressing Cancers Using Single Photon Emission Computed Tomography-Computed Tomography (Spect-Ct) Imaging. *Oncotarget.* 2015; 6:4496–4504. [PubMed: 25756664]
88. Leconet W, Larbouret C, Charde T, Thomas G, Neiveyans M, Busson M, Jarlier M, Radosevic-Robin N, Pugnieri M, Bernex F, Penault-Llorca F, Pasquet JM, Pelegrin A, Robert B. Preclinical Validation of Axl Receptor as a Target for Antibody-Based Pancreatic Cancer Immunotherapy. *Oncogene.* 2014; 33:5405–5414. [PubMed: 24240689]
89. Song X, Wang H, Logsdon CD, Rashid A, Fleming JB, Abbruzzese JL, Gomez HF, Evans DB, Wang H. Overexpression of Receptor Tyrosine Kinase Axl Promotes Tumor Cell Invasion and Survival in Pancreatic Ductal Adenocarcinoma. *Cancer.* 2011; 117:734–743. [PubMed: 20922806]
90. Sabbah EN, Kadouche J, Ellison D, Finucane C, Decaudin D, Mather SJ. In Vitro and in Vivo Comparison of Dtpa- and Dota-Conjugated Antiferritin Monoclonal Antibody for Imaging and Therapy of Pancreatic Cancer. *Nucl Med Biol.* 2007; 34:293–304. [PubMed: 17383579]
91. Sawada T, Nishihara T, Yamamoto A, Teraoka H, Yamashita Y, Okamura T, Ochi H, Ho JJ, Kim YS, Hirakawa K. Preoperative Clinical Radioimmunodetection of Pancreatic Cancer by 111In-Labeled Chimeric Monoclonal Antibody Nd2. *Jpn J Cancer Res.* 1999; 90:1179–1186. [PubMed: 10595748]
92. Kufe DW. Mucins in Cancer: Function, Prognosis and Therapy. *Nat Rev Cancer.* 2009; 9:874–885. [PubMed: 19935676]
93. Kaur S, Kumar S, Momi N, Sasson AR, Batra SK. Mucins in Pancreatic Cancer and Its Microenvironment. *Nat Rev Gastroenterol Hepatol.* 2013; 10:607–620. [PubMed: 23856888]
94. Foss CA, Fox JJ, Feldmann G, Maitra A, Iacobuzio-Donohue C, Kern SE, Hruban R, Pomper MG. Radiolabeled Anti-Claudin 4 and Anti-Prostate Stem Cell Antigen: Initial Imaging in Experimental Models of Pancreatic Cancer. *Mol Imaging.* 2007; 6:131–139. [PubMed: 17445507]
95. Michl P, Buchholz M, Rolke M, Kunsch S, Lohr M, McClane B, Tsukita S, Leder G, Adler G, Gress TM. Claudin-4: A New Target for Pancreatic Cancer Treatment Using Clostridium Perfringens Enterotoxin. *Gastroenterology.* 2001; 121:678–684. [PubMed: 11522752]
96. Nichols LS, Ashfaq R, Iacobuzio-Donahue CA. Claudin 4 Protein Expression in Primary and Metastatic Pancreatic Cancer: Support for Use as a Therapeutic Target. *Am J Clin Pathol.* 2004; 121:226–230. [PubMed: 14983936]
97. Leung, K. *Molecular Imaging and Contrast Agent Database (Micad)*. Bethesda (MD): 2004. 111In-P-Benzyl Isothiocyanate-1,4,7,10-Tetraazacyclododecane-1,4,7,10-Tetraacetic Acid-14c5 Monoclonal Antibody.
98. Vervoort L, Burvenich I, Staelens S, Dumolyn C, Waegemans E, Van Steenkiste M, Baird SK, Scott AM, De Vos F. Preclinical Evaluation of Monoclonal Antibody 14c5 for Targeting Pancreatic Cancer. *Cancer Biother Radiopharm.* 2010; 25:193–205. [PubMed: 20423233]
99. Erickson JJ. Development of the Scintillation Camera. *Am J Physiol Imaging.* 1992; 7:98–104. [PubMed: 1343222]
100. Stefanovic L. the Beginnings and Development of Diagnostic Imaging in Nuclear Medicine. *Med Pregl.* 2001; 54:289–296. [PubMed: 11759228]



101. Kaufmann LW, Vaillant JC, van Gulik TM, van Royen EA, Parc R, Obertop H. Efficacy of Monoclonal Antibody 131i-B72.3 Immunoscintigraphy of Pancreatic Adenocarcinoma Xenografts in Nude Mice. *Eur J Surg*. 1999; 165:659–664. [PubMed: 10452260]
102. Otsuji E, Yamaguchi T, Yamaoka N, Kato M, Kotani T, Kitamura K, Yamaguchi N, Takahashi T. Enhanced Tumor Localization of Radiolabeled Fab Fragments of Monoclonal Antibody A7 in Nude Mice Bearing Human Pancreatic Carcinoma Xenografts. *Jpn J Cancer Res*. 1993; 84:914–920. [PubMed: 8407556]
103. Otsuji E, Matsumura H, Okamoto K, Toma A, Kuriu Y, Ichikawa D, Hagiwara A, Yamagishi H. Application of 99mTc Labeled Chimeric Fab Fragments of Monoclonal Antibody A7 for Immunoscintigraphy of Pancreatic Carcinoma. *J Surg Oncol*. 2003; 84:160–165. [PubMed: 14598360]
104. Scherzinger AL, Hendee WR. Basic Principles of Magnetic Resonance Imaging--an Update. *West J Med*. 1985; 143:782–792. [PubMed: 3911591]
105. Plewes DB, Kucharczyk W. Physics of MRI: A Primer. *J Magn Reson Imaging*. 2012; 35:1038–1054. [PubMed: 22499279]
106. Jasanoff A. MRI Contrast Agents for Functional Molecular Imaging of Brain Activity. *Curr Opin Neurobiol*. 2007; 17:593–600. [PubMed: 18093824]
107. Kartalis N, Mucelli RM, Sundin A. Recent Developments in Imaging of Pancreatic Neuroendocrine Tumors. *Ann Gastroenterol*. 2015; 28:193–202. [PubMed: 25830417]
108. Kalra MK, Maher MM, Mueller PR, Saini S. State-of-the-Art Imaging of Pancreatic Neoplasms. *Br J Radiol*. 2003; 76:857–865. [PubMed: 14711772]
109. Raman SP, Horton KM, Fishman EK. Multimodality Imaging of Pancreatic Cancer--Computed Tomography, Magnetic Resonance Imaging, and Positron Emission Tomography. *Cancer J*. 2012; 18:511–522. [PubMed: 23187837]
110. Grimm J, Potthast A, Wunder A, Moore A. Magnetic Resonance Imaging of the Pancreas and Pancreatic Tumors in a Mouse Orthotopic Model of Human Cancer. *Int J Cancer*. 2003; 106:806–811. [PubMed: 12866043]
111. Deng L, Ke X, He Z, Yang D, Gong H, Zhang Y, Jing X, Yao J, Chen J. A Msln-Targeted Multifunctional Nanoimmunoliposome for MRI and Targeting Therapy in Pancreatic Cancer. *Int J Nanomedicine*. 2012; 7:5053–5065. [PubMed: 23028227]
112. Yoon HY, Saravanakumar G, Heo R, Choi SH, Song IC, Han MH, Kim K, Park JH, Choi K, Kwon IC, Park K. Hydrotropic Magnetic Micelles for Combined Magnetic Resonance Imaging and Cancer Therapy. *J Control Release*. 2012; 160:692–698. [PubMed: 22543013]
113. Lim EK, Kim T, Paik S, Haam S, Huh YM, Lee K. Nanomaterials for Theranostics: Recent Advances and Future Challenges. *Chem Rev*. 2015; 115:327–394. [PubMed: 25423180]
114. Wang X, Xing X, Zhang B, Liu F, Cheng Y, Shi D. Surface Engineered Antifouling Optomagnetic Spions for Bimodal Targeted Imaging of Pancreatic Cancer Cells. *Int J Nanomedicine*. 2014; 9:1601–1615. [PubMed: 24741308]
115. Fei LM, Wang CL, Zhao WH, Cui K, Zhang B, Zhou WY, Zhong WX, Li S. Quantitative Analysis and Significance of Cxcl12 and Cxcr4 Expression with Lymphangiogenesis of Pancreatic Adenocarcinoma. *Zhonghua Wai Ke Za Zhi*. 2009; 47:783–786. [PubMed: 19615218]
116. Mori T, Doi R, Koizumi M, Toyoda E, Ito D, Kami K, Masui T, Fujimoto K, Tamamura H, Hiramatsu K, Fujii N, Imamura M. Cxcr4 Antagonist Inhibits Stromal Cell-Derived Factor 1-Induced Migration and Invasion of Human Pancreatic Cancer. *Mol Cancer Ther*. 2004; 3:29–37. [PubMed: 14749473]
117. Marchesi F, Monti P, Leone BE, Zerbi A, Vecchi A, Piemonti L, Mantovani A, Allavena P. Increased Survival, Proliferation, and Migration in Metastatic Human Pancreatic Tumor Cells Expressing Functional Cxcr4. *Cancer Res*. 2004; 64:8420–8427. [PubMed: 15548713]
118. He Y, Song W, Lei J, Li Z, Cao J, Huang S, Meng J, Xu H, Jin Z, Xue H. Anti-Cxcr4 Monoclonal Antibody Conjugated to Ultrasmall Superparamagnetic Iron Oxide Nanoparticles in an Application of MRI Molecular Imaging of Pancreatic Cancer Cell Lines. *Acta Radiol*. 2012; 53:1049–1058. [PubMed: 23012484]

119. Thomas RM, Kim J, Revelo-Penafiel MP, Angel R, Dawson DW, Lowy AM. The Chemokine Receptor Cxcr4 Is Expressed in Pancreatic Intraepithelial Neoplasia. *Gut*. 2008; 57:1555–1560. [PubMed: 18664506]
120. Yang L, Mao H, Wang YA, Cao Z, Peng X, Wang X, Duan H, Ni C, Yuan Q, Adams G, Smith MQ, Wood WC, Gao X, Nie S. Single Chain Epidermal Growth Factor Receptor Antibody Conjugated Nanoparticles for in Vivo Tumor Targeting and Imaging. *Small*. 2009; 5:235–243. [PubMed: 19089838]
121. Xie D, Xie K. Pancreatic Cancer Stromal Biology and Therapy. *Genes Dis*. 2015; 2:133–143. [PubMed: 26114155]
122. Pirolo KF, Dagata J, Wang P, Freedman M, Vldar A, Fricke S, Ileva L, Zhou Q, Chang EH. A Tumor-Targeted Nanodelivery System to Improve Early Mri Detection of Cancer. *Mol Imaging*. 2006; 5:41–52. [PubMed: 16779969]
123. Chen W, Ayala-Orozco C, Biswal NC, Perez-Torres C, Bartels M, Bardhan R, Stinnet G, Liu XD, Ji B, Deorukhkar A, Brown LV, Guha S, Pautler RG, Krishnan S, Halas NJ, Joshi A. Targeting Pancreatic Cancer with Magneto-Fluorescent Theranostic Gold Nanoshells. *Nanomedicine (Lond)*. 2014; 9:1209–1222. [PubMed: 24063415]
124. Moniaux N, Chakraborty S, Yalniz M, Gonzalez J, Shostrom VK, Standop J, Lele SM, Ouellette M, Pour PM, Sasson AR, Brand RE, Hollingsworth MA, Jain M, Batra SK. Early Diagnosis of Pancreatic Cancer: Neutrophil Gelatinase-Associated Lipocalin as a Marker of Pancreatic Intraepithelial Neoplasia. *Br J Cancer*. 2008; 98:1540–1547. [PubMed: 18392050]
125. Kherlopian AR, Song T, Duan Q, Neimark MA, Po MJ, Gohagan JK, Laine AF. A Review of Imaging Techniques for Systems Biology. *BMC Syst Biol*. 2008; 2:74. [PubMed: 18700030]
126. Balas C. Review of Biomedical Optical Imaging—a Powerful, Non-Invasive, Non-Ionizing Technology for Improving in Vivo Diagnosis. *Meas Sci Technol*. 2009; 20
127. Robinson JT, Hong G, Liang Y, Zhang B, Yaghi OK, Dai H. In Vivo Fluorescence Imaging in the Second near-Infrared Window with Long Circulating Carbon Nanotubes Capable of Ultrahigh Tumor Uptake. *J Am Chem Soc*. 2012; 134:10664–10669. [PubMed: 22667448]
128. Smith AM, Mancini MC, Nie S. Bioimaging: Second Window for in Vivo Imaging. *Nat Nanotechnol*. 2009; 4:710–711. [PubMed: 19898521]
129. Patel AR, Lim E, Francis KP, Singh M. Opening up the Optical Imaging Window Using Nano-Luciferin. *Pharm Res*. 2014; 31:3073–3084. [PubMed: 24831312]
130. Pansare V, Hejazi S, Faenza W, Prud'homme RK. Review of Long-Wavelength Optical and NIR Imaging Materials: Contrast Agents, Fluorophores and Multifunctional Nano Carriers. *Chem Mater*. 2012; 24:812–827. [PubMed: 22919122]
131. Tran Cao HS, Kaushal S, Metildi CA, Menen RS, Lee C, Snyder CS, Messer K, Pu M, Luiken GA, Talamini MA, Hoffman RM, Bouvet M. Tumor-Specific Fluorescence Antibody Imaging Enables Accurate Staging Laparoscopy in an Orthotopic Model of Pancreatic Cancer. *Hepatogastroenterology*. 2012; 59:1994–1999. [PubMed: 22369743]
132. Kaushal S, McElroy MK, Luiken GA, Talamini MA, Moossa AR, Hoffman RM, Bouvet M. Fluorophore-Conjugated Anti-Cea Antibody for the Intraoperative Imaging of Pancreatic and Colorectal Cancer. *J Gastrointest Surg*. 2008; 12:1938–1950. [PubMed: 18665430]
133. Tran Cao HS, Kaushal S, Lee C, Snyder CS, Thompson KJ, Horgan S, Talamini MA, Hoffman RM, Bouvet M. Fluorescence Laparoscopy Imaging of Pancreatic Tumor Progression in an Orthotopic Mouse Model. *Surg Endosc*. 2011; 25:48–54. [PubMed: 20533064]
134. Boonstra MC, Tolner B, Schaafsma BE, Boogerd LS, Prevoo HA, Bhavsar G, Kuppen PJ, Sier CF, Bonsing BA, Frangioni JV, van de Velde CJ, Chester KA, Vahrmeijer AL. Preclinical Evaluation of a Novel Cea-Targeting near-Infrared Fluorescent Tracer Delineating Colorectal and Pancreatic Tumors. *Int J Cancer*. 2015; 137:1910–1920. [PubMed: 25895046]
135. Boehm MK, Corper AL, Wan T, Sohi MK, Sutton BJ, Thornton JD, Keep PA, Chester KA, Begent RH, Perkins SJ. Crystal Structure of the Anti-(Carcinoembryonic Antigen) Single-Chain Fv Antibody Mfe-23 and a Model for Antigen Binding Based on Intermolecular Contacts. *Biochem J*. 2000; 346(Pt 2):519–528. [PubMed: 10677374]
136. Hiroshima Y, Maawy A, Zhang Y, Murakami T, Momiyama M, Mori R, Matsuyama R, Chishima T, Tanaka K, Ichikawa Y, Endo I, Hoffman RM, Bouvet M. Fluorescence-Guided Surgery, but

- Not Bright-Light Surgery, Prevents Local Recurrence in a Pancreatic Cancer Patient Derived Orthotopic Xenograft (Pdox) Model Resistant to Neoadjuvant Chemotherapy (Nac). *Pancreatology*. 2015; 15:295–301. [PubMed: 25800176]
137. Maawy AA, Hiroshima Y, Zhang Y, Garcia-Guzman M, Luiken GA, Kobayashi H, Hoffman RM, Bouvet M. Photoimmunotherapy Lowers Recurrence after Pancreatic Cancer Surgery in Orthotopic Nude Mouse Models. *J Surg Res*. 2015; 197:5–11. [PubMed: 25799527]
138. Bouvet M, Hoffman RM. Fluorescence-Guided Surgery: It Is the Cure That Matters: In Reply to Giorgakis and Colleagues. *J Am Coll Surg*. 2015; 220:377–379. [PubMed: 25700908]
139. Maawy AA, Hiroshima Y, Zhang Y, Luiken GA, Hoffman RM, Bouvet M. Specific Tumor Labeling Enhanced by Polyethylene Glycol Linkage of near Infrared Dyes Conjugated to a Chimeric Anti-Carcinoembryonic Antigen Antibody in a Nude Mouse Model of Human Pancreatic Cancer. *J Biomed Opt*. 2014; 19:101504. [PubMed: 24887695]
140. Metildi CA, Kaushal S, Luiken GA, Hoffman RM, Bouvet M. Advantages of Fluorescence-Guided Laparoscopic Surgery of Pancreatic Cancer Labeled with Fluorescent Anti-Carcinoembryonic Antigen Antibodies in an Orthotopic Mouse Model. *J Am Coll Surg*. 2014; 219:132–141. [PubMed: 24768506]
141. Metildi CA, Kaushal S, Lee C, Hardamon CR, Snyder CS, Luiken GA, Talamini MA, Hoffman RM, Bouvet M. An Led Light Source and Novel Fluorophore Combinations Improve Fluorescence Laparoscopic Detection of Metastatic Pancreatic Cancer in Orthotopic Mouse Models. *J Am Coll Surg*. 2012; 214:997–1007. e1002. [PubMed: 22542065]
142. Wu E, Zhou S, Bhat K, Ma Q. Ca 19-9 and Pancreatic Cancer. *Clinical advances in hematology & oncology: H&O*. 2013; 11:53–55. [PubMed: 23596673]
143. Ballehaninna UK, Chamberlain RS. Serum Ca 19-9 as a Biomarker for Pancreatic Cancer—a Comprehensive Review. *Indian J Surg Oncol*. 2011; 2:88–100. [PubMed: 22693400]
144. McElroy M, Kaushal S, Luiken GA, Talamini MA, Moossa AR, Hoffman RM, Bouvet M. Imaging of Primary and Metastatic Pancreatic Cancer Using a Fluorophore-Conjugated Anti-Ca19-9 Antibody for Surgical Navigation. *World J Surg*. 2008; 32:1057–1066. [PubMed: 18264829]
145. Hiroshima Y, Maawy A, Zhang Y, Murakami T, Momiyama M, Mori R, Matsuyama R, Katz MH, Fleming JB, Chishima T, Tanaka K, Ichikawa Y, Endo I, Hoffman RM, Bouvet M. Metastatic Recurrence in a Pancreatic Cancer Patient Derived Orthotopic Xenograft (Pdox) Nude Mouse Model Is Inhibited by Neoadjuvant Chemotherapy in Combination with Fluorescence-Guided Surgery with an Anti-Ca 19-9-Conjugated Fluorophore. *PLoS One*. 2014; 9:e114310. [PubMed: 25463150]
146. Bunger S, Laubert T, Roblick UJ, Habermann JK. Serum Biomarkers for Improved Diagnostic of Pancreatic Cancer: A Current Overview. *J Cancer Res Clin Oncol*. 2011; 137:375–389. [PubMed: 21193998]
147. Qu CF, Li Y, Song YJ, Rizvi SM, Raja C, Zhang D, Samra J, Smith R, Perkins AC, Apostolidis C, Allen BJ. Muc1 Expression in Primary and Metastatic Pancreatic Cancer Cells for in Vitro Treatment by (213)Bi-C595 Radioimmunoconjugate. *Br J Cancer*. 2004; 91:2086–2093. [PubMed: 15599383]
148. Bafna S, Kaur S, Batra SK. Membrane-Bound Mucins: The Mechanistic Basis for Alterations in the Growth and Survival of Cancer Cells. *Oncogene*. 2010; 29:2893–2904. [PubMed: 20348949]
149. Park JY, Hiroshima Y, Lee JY, Maawy AA, Hoffman RM, Bouvet M. Muc1 Selectively Targets Human Pancreatic Cancer in Orthotopic Nude Mouse Models. *PLoS One*. 2015; 10:e0122100. [PubMed: 25815753]
150. Kosaka N, McCann TE, Mitsunaga M, Choyke PL, Kobayashi H. Real-Time Optical Imaging Using Quantum Dot and Related Nanocrystals. *Nanomedicine (Lond)*. 2010; 5:765–776.
151. Yong KT, Ding H, Roy I, Law WC, Bergey EJ, Maitra A, Prasad PN. Imaging Pancreatic Cancer Using Bioconjugated Inp Quantum Dots. *ACS nano*. 2009; 3:502–510. [PubMed: 19243145]
152. Chen N, He Y, Su Y, Li X, Huang Q, Wang H, Zhang X, Tai R, Fan C. The Cytotoxicity of Cadmium-Based Quantum Dots. *Biomaterials*. 2012; 33:1238–1244. [PubMed: 22078811]

153. Kampmeier F, Niesen J, Koers A, Ribbert M, Brecht A, Fischer R, Kiessling F, Barth S, Thepen T. Rapid Optical Imaging of Egf Receptor Expression with a Single-Chain Antibody Snap-Tag Fusion Protein. *Eur J Nucl Med Mol Imaging*. 2010; 37:1926–1934. [PubMed: 20449589]
154. Bowen T. Radiation-Induced Thermoacoustic Soft-Tissue Imaging. *Ieee T Son Ultrason*. 1982; 29:187–187.
155. Fan Y, Mandelis A, Spirou G, Vitkin IA. Development of a Laser Photothermal Acoustic Frequency-Swept System for Subsurface Imaging: Theory and Experiment. *J Acoust Soc Am*. 2004; 116:3523–3533. [PubMed: 15658704]
156. Lashkari B, Mandelis A. Photoacoustic Radar Imaging Signal-to-Noise Ratio, Contrast, and Resolution Enhancement Using Nonlinear Chirp Modulation. *Opt Lett*. 2010; 35:1623–1625. [PubMed: 20479829]
157. Maslov K, Wang LV. Photoacoustic Imaging of Biological Tissue with Intensity-Modulated Continuous-Wave Laser. *J Biomed Opt*. 2008; 13:024006. [PubMed: 18465969]
158. Dovlo E, Lashkari B, Mandelis A, Shi W, Liu FF. Photoacoustic Radar Phase-Filtered Spatial Resolution and Co-Registered Ultrasound Image Enhancement for Tumor Detection. *Biomed Opt Express*. 2015; 6:1003–1009. [PubMed: 25798321]
159. Taruttis A, Ntziachristos V. Advances in Real-Time Multispectral Photoacoustic Imaging and Its Applications. *Nat Photonics*. 2015; 9:219–227.
160. Wang LV, Hu S. Photoacoustic Tomography: In Vivo Imaging from Organelles to Organs. *Science*. 2012; 335:1458–1462. [PubMed: 22442475]
161. Xia J, Yao J, Wang LV. Photoacoustic Tomography: Principles and Advances. *Electromagn Waves (Camb)*. 2014; 147:1–22. [PubMed: 25642127]
162. Xia J, Wang LV. Small-Animal Whole-Body Photoacoustic Tomography: A Review. *IEEE Trans Biomed Eng*. 2014; 61:1380–1389. [PubMed: 24108456]
163. Beard P. Biomedical Photoacoustic Imaging. 2011; 1:602–631.
164. Nie L, Wang S, Wang X, Rong P, Ma Y, Liu G, Huang P, Lu G, Chen X. In Vivo Volumetric Photoacoustic Molecular Angiography and Therapeutic Monitoring with Targeted Plasmonic Nanostars. *Small*. 2014; 10:1585–1593. 1441. [PubMed: 24150920]
165. Kruger RA, Lam RB, Reinecke DR, Del Rio SP, Doyle RP. Photoacoustic Angiography of the Breast. *Med Phys*. 2010; 37:6096–6100. [PubMed: 21158321]
166. Wang X, Ku G, Wegiel MA, Bornhop DJ, Stoica G, Wang LV. Noninvasive Photoacoustic Angiography of Animal Brains in Vivo with near-Infrared Light and an Optical Contrast Agent. *Opt Lett*. 2004; 29:730–732. [PubMed: 15072373]
167. Kim C, Favazza C, Wang LV. In Vivo Photoacoustic Tomography of Chemicals: High-Resolution Functional and Molecular Optical Imaging at New Depths. *Chem Rev*. 2010; 110:2756–2782. [PubMed: 20210338]
168. Lakshman M, Needles A. Screening and Quantification of the Tumor Microenvironment with Micro-Ultrasound and Photoacoustic Imaging. *Nat Meth*. 2015; 12
169. Homan KA, Souza M, Truby R, Luke GP, Green C, Vreeland E, Emelianov S. Silver Nanoplate Contrast Agents for in Vivo Molecular Photoacoustic Imaging. *ACS nano*. 2012; 6:641–650. [PubMed: 22188516]
170. Homan K, Shah J, Gomez S, Gensler H, Karpouk A, Brannon-Peppas L, Emelianov S. Combined Ultrasound and Photoacoustic Imaging of Pancreatic Cancer Using Nanocage Contrast Agents. *P Soc Photo-Opt Ins*. 2009; 7177
171. Hudson SV, Huang JS, Yin W, Albeituni S, Rush J, Khanal A, Yan J, Ceresa BP, Frieboes HB, McNally LR. Targeted Noninvasive Imaging of Egfr-Expressing Orthotopic Pancreatic Cancer Using Multispectral Photoacoustic Tomography. *Cancer Res*. 2014; 74:6271–6279. [PubMed: 25217521]
172. Xu J, Cai X, Yao J, Dirk S, Zeng C, Hawkins WG, Wang LV, Mach RH. Abstract 356: Photoacoustic Imaging of Pancreatic Cancer Proliferation Via Sigma-2 Receptor/Pgrmc1-Eyfp. *Cancer Res*. 2014; 72:356–356.
173. Junttila MR, de Sauvage FJ. Influence of Tumour Micro-Environment Heterogeneity on Therapeutic Response. *Nature*. 2013; 501:346–354. [PubMed: 24048067]

174. Chen F, Nayak TR, Goel S, Valdovinos HF, Hong H, Theuer CP, Barnhart TE, Cai W. In Vivo Tumor Vasculature Targeted Pet/Nirf Imaging with Trc105(Fab)-Conjugated, Dual-Labeled Mesoporous Silica Nanoparticles. *Mol Pharm*. 2014; 11:4007–4014. [PubMed: 24937108]
175. Hong H, Severin GW, Yang Y, Engle JW, Zhang Y, Barnhart TE, Liu G, Leigh BR, Nickles RJ, Cai W. Positron Emission Tomography Imaging of Cd105 Expression with 89zr-Df-Trc105. *Eur J Nucl Med Mol Imaging*. 2012; 39:138–148. [PubMed: 21909753]
176. Hiraoka N, Ino Y, Sekine S, Tsuda H, Shimada K, Kosuge T, Zavada J, Yoshida M, Yamada K, Koyama T, Kanai Y. Tumour Necrosis Is a Postoperative Prognostic Marker for Pancreatic Cancer Patients with a High Interobserver Reproducibility in Histological Evaluation. *Br J Cancer*. 2010; 103:1057–1065. [PubMed: 20736942]
177. Liu JK. The History of Monoclonal Antibody Development - Progress, Remaining Challenges and Future Innovations. *Ann Med Surg (Lond)*. 2014; 3:113–116. [PubMed: 25568796]
178. Velpandian T, Sharma C, Garg SP, Mandal S, Ghose S. Safety and Cost-Effectiveness of Single Dose Dispensing of Bevacizumab for Various Retinal Pathologies in Developing Countries. *Indian J Ophthalmol*. 2007; 55:488–490. [PubMed: 17951922]
179. Hidalgo M. New Insights into Pancreatic Cancer Biology. *Ann Oncol*. 2012; 23(Suppl 10):x135–138. [PubMed: 22987949]
180. Irie H, Honda H, Kaneko K, Kuroiwa T, Yoshimitsu K, Masuda K. Comparison of Helical Ct and Mr Imaging in Detecting and Staging Small Pancreatic Adenocarcinoma. *Abdom Imaging*. 1997; 22:429–433. [PubMed: 9157866]
181. Francis IR. Role of Ct and Mr in Detection and Staging of Pancreatic Adenocarcinoma. *Cancer Imaging*. 2004; 4:10–14. [PubMed: 18211854]
182. Saisho H, Yamaguchi T. Diagnostic Imaging for Pancreatic Cancer: Computed Tomography, Magnetic Resonance Imaging, and Positron Emission Tomography. *Pancreas*. 2004; 28:273–278. [PubMed: 15084970]
183. Malak M, Masuda D, Ogura T, Imoto A, Abdelaal UM, Sabet EA, Abo Dahab LH, Higuchi K. Yield of Endoscopic Ultrasound-Guided Fine Needle Aspiration and Endoscopic Retrograde Cholangiopancreatography for Solid Pancreatic Neoplasms. *Scand J Gastroenterol*. 2015:1–8.
184. Pietryga JA, Morgan DE. Imaging Preoperatively for Pancreatic Adenocarcinoma. *J Gastrointest Oncol*. 2015; 6:343–357. [PubMed: 26261722]
185. Tummala P, Junaidi O, Agarwal B. Imaging of Pancreatic Cancer: An Overview. *J Gastrointest Oncol*. 2011; 2:168–174. [PubMed: 22811847]
186. Klauss M, Maier-Hein K, Tjaden C, Hackert T, Grenacher L, Stieltjes B. Ivim Dw-Mri of Autoimmune Pancreatitis: Therapy Monitoring and Differentiation from Pancreatic Cancer. *Eur Radiol*. 2015
187. Serrano OK, Chaudhry MA, Leach SD. The Role of Pet Scanning in Pancreatic Cancer. *Adv Surg*. 2010; 44:313–325. [PubMed: 20919529]
188. De Paoli P. Institutional Shared Resources and Translational Cancer Research. *J Transl Med*. 2009; 7:54. [PubMed: 19563639]
189. Sevvick-Muraca EM, Akers WJ, Joshi BP, Luker GD, Cutler CS, Marnett LJ, Contag CH, Wang TD, Azhdarinia A. Advancing the Translation of Optical Imaging Agents for Clinical Imaging. *Biomed Opt Express*. 2013; 4:160–170. [PubMed: 23304655]
190. Phillips E, Penate-Medina O, Zanzonico PB, Carvajal RD, Mohan P, Ye Y, Humm J, Gonen M, Kalaigian H, Schoder H, Strauss HW, Larson SM, Wiesner U, Bradbury MS. Clinical Translation of an Ultrasmall Inorganic Optical-Pet Imaging Nanoparticle Probe. *Sci Transl Med*. 2014; 6:260ra149.
191. Ntziachristos V. Clinical Translation of Optical and Optoacoustic Imaging. *Philos Trans A Math Phys Eng Sci*. 2011; 369:4666–4678. [PubMed: 22006913]
192. Roshan MV, Razaghi S, Asghari F, Rawat RS, Springham SV, Lee P, Lee S, Tan TL. Potential Medical Applications of the Plasma Focus in the Radioisotope Production for Pet Imaging. *Phys Lett A*. 2014; 378:2168–2170.
193. Muehllehner G, Karp JS. Positron Emission Tomography. *Phys Med Biol*. 2006; 51:R117–137. [PubMed: 16790899]

194. Moses WW. Fundamental Limits of Spatial Resolution in Pet. Nucl Instrum Methods Phys Res A. 2011; 648(Supplement 1):S236–S240. [PubMed: 21804677]
195. Surti S, Scheuermann R, Werner ME, Karp JS. Improved Spatial Resolution in Pet Scanners Using Sampling Techniques. IEEE Trans Nucl Sci. 2009; 56:596–601. [PubMed: 19779586]
196. Chaudhary V, Bano S. Imaging of the Pancreas: Recent Advances. Indian J Endocrinol Metab. 2011; 15:S25–32. [PubMed: 21847450]
197. Mitchell GS, Cherry SR. A High-Sensitivity Small Animal Spect System. Phys Med Biol. 2009; 54:1291–1305. [PubMed: 19190360]
198. Ding H, Wu F. Image Guided Biodistribution and Pharmacokinetic Studies of Theranostics. Theranostics. 2012; 2:1040–1053. [PubMed: 23227121]
199. Key J, Leary JF. Nanoparticles for Multimodal in Vivo Imaging in Nanomedicine. Int J Nanomedicine. 2014; 9:711–726. [PubMed: 24511229]
200. Schultz-Sikma, EA.; Meade, TJ. Supramol Chem. John Wiley & Sons, Ltd; 2012. Supramolecular Chemistry in Biological Imaging in Vivo.
201. Stephen ZR, Kievit FM, Zhang M. Magnetite Nanoparticles for Medical Mr Imaging. Mater Today (Kidlington). 2011; 14:330–338. [PubMed: 22389583]
202. Cai W. Seeing Is Believing: Molecular Imaging in Living Subjects. Curr Pharm Biotechnol. 2010; 11:544. [PubMed: 20687893]
203. Massoud TF, Gambhir SS. Molecular Imaging in Living Subjects: Seeing Fundamental Biological Processes in a New Light. Genes Dev. 2003; 17:545–580. [PubMed: 12629038]
204. Lacroix LM, Delpech F, Nayral C, Lachaize S, Chaudret B. New Generation of Magnetic and Luminescent Nanoparticles for in Vivo Real-Time Imaging. Interface Focus. 2013; 3:20120103. [PubMed: 24427542]
205. Bohndiek SE, Bodapati S, Van De Sompel D, Kothapalli SR, Gambhir SS. Development and Application of Stable Phantoms for the Evaluation of Photoacoustic Imaging Instruments. PLoS One. 2013; 8:e75533. [PubMed: 24086557]
206. Ku G, Wang LV. Deeply Penetrating Photoacoustic Tomography in Biological Tissues Enhanced with an Optical Contrast Agent. Opt Lett. 2005; 30:507–509. [PubMed: 15789718]
207. Ntziachristos V. Going Deeper Than Microscopy: The Optical Imaging Frontier in Biology. Nat Methods. 2010; 7:603–614. [PubMed: 20676081]
208. Zhang Y, Jeon M, Rich LJ, Hong H, Geng J, Zhang Y, Shi S, Barnhart TE, Alexandridis P, Huiying JD, Seshadri M, Cai W, Kim C, Lovell JF. Non-Invasive Multimodal Functional Imaging of the Intestine with Frozen Micellar Naphthalocyanines. Nat Nanotechnol. 2014; 9:631–638. [PubMed: 24997526]
209. Zhu X, Li J, Hong Y, Kimura RH, Ma X, Liu H, Qin C, Hu X, Hayes TR, Benny P, Gambhir SS, Cheng Z. 99mTc-Labeled Cystine Knot Peptide Targeting Integrin  $\alpha v\beta 6$  for Tumor Spect Imaging. Mol Pharm. 2014; 11:1208–1217. [PubMed: 24524409]
210. Cruz-Monserrate Z, Roland CL, Deng D, Arumugam T, Moshnikova A, Andreev OA, Reshetnyak YK, Logsdon CD. Targeting Pancreatic Ductal Adenocarcinoma Acidic Microenvironment. Sci Rep. 2014; 4:4410. [PubMed: 24642931]
211. Knoop K, Kolokythas M, Klutz K, Willhauck MJ, Wunderlich N, Draganovici D, Zach C, Gildehaus FJ, Boning G, Goke B, Wagner E, Nelson PJ, Spitzweg C. Image-Guided, Tumor Stroma-Targeted  $^{131}\text{I}$  Therapy of Hepatocellular Cancer after Systemic Mesenchymal Stem Cell-Mediated Nis Gene Delivery. Mol Ther. 2011; 19:1704–1713. [PubMed: 21587211]

### Construction of Antibody-based Imaging Agents

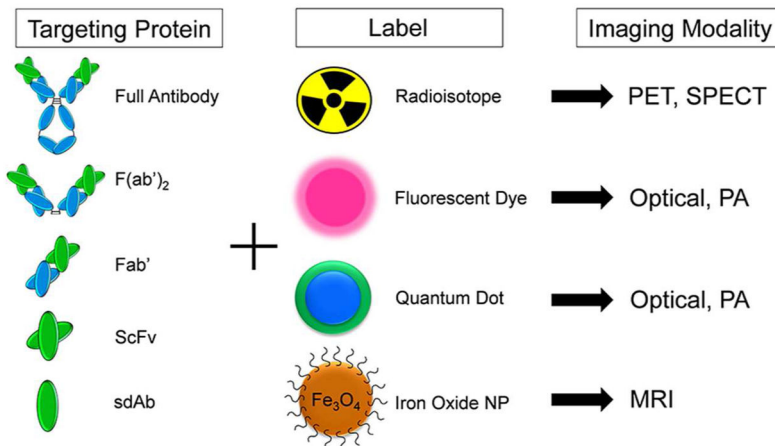


**Figure 1.** Construction of an antibody-based molecular imaging probe requires a contrast agent specific for the imaging modality. Full and fragmented antibodies may be employed as targeting agents. Some examples of antibody fragments include F(ab')<sub>2</sub>, Fab, single-chain variable fragment (ScFv), and nanobody (sdAb). Radioisotopes are employed for positron emission tomography (PET) and single-photon emission computed tomography (SPECT) imaging. Fluorescent dyes and quantum dots are utilized for optical and photoacoustic (PA) imaging. Magnetic (e.g., iron oxide) nanoparticles are commonly used in magnetic resonance imaging (MRI).

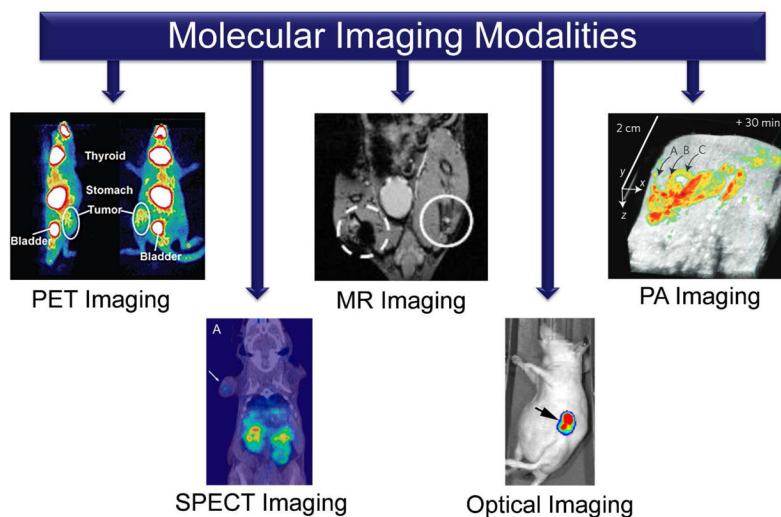


**Figure 2.** Five molecular imaging modalities employed for cancer screening and therapeutic monitoring includes positron emission tomography (PET), single-photon emission computed tomography (SPECT), magnetic resonance (MR), optical, and photoacoustic (PA) imaging. Adapted from Ref. <sup>208–211</sup> with permission.



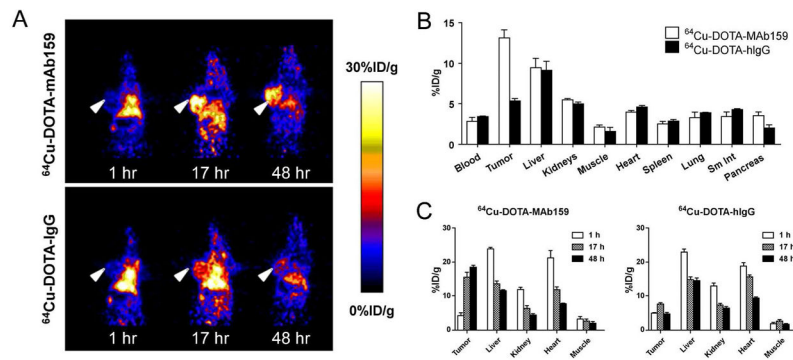


**Figure 3.** PET imaging of GRP78 overexpression in pancreatic cancer xenograft model. (A) PET images were decay corrected, with 3 time points shown at 1, 17, and 48 hr post-injection of  $^{64}\text{Cu}$ -DOTA-MAb159 (targeting GRP78) or  $^{64}\text{Cu}$ -DOTA-IgG (control). (B) Biodistribution of  $^{64}\text{Cu}$ -DOTA-MAb159 and  $^{64}\text{Cu}$ -DOTA-IgG, through direct tissue sampling, at 48 hr post-injection. (C) PET quantification of  $^{64}\text{Cu}$ -DOTA-MAb159 and  $^{64}\text{Cu}$ -DOTA-IgG in major organs at three imaging time points (1, 17, and 48 hr). Adapted from Ref. <sup>49</sup> with permission.

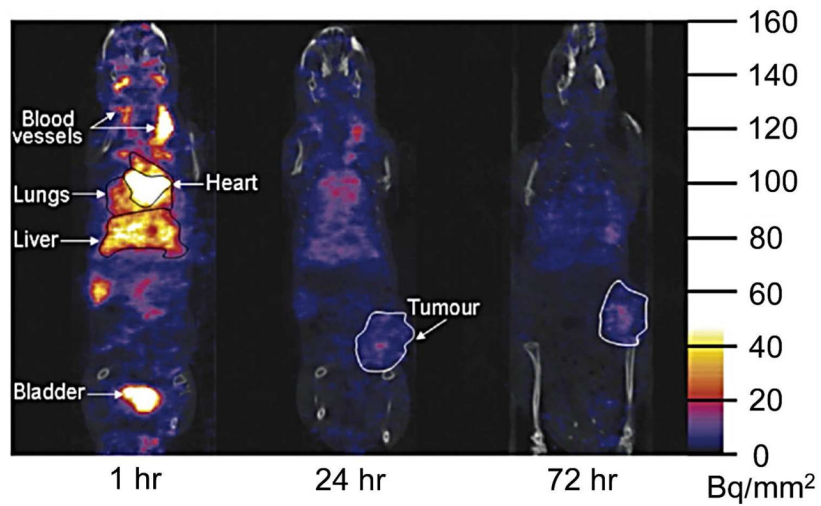


**Figure 4.** SPECT imaging of ferritin expression in pancreatic cancer using the novel antibody AMB8LK. CAPAN-1 xenograft mice were injected with <sup>111</sup>In-DTPA-AMB8LK and imaged at 1, 24, and 72 hr post-injection. Adapted from Ref. <sup>90</sup> with permission.

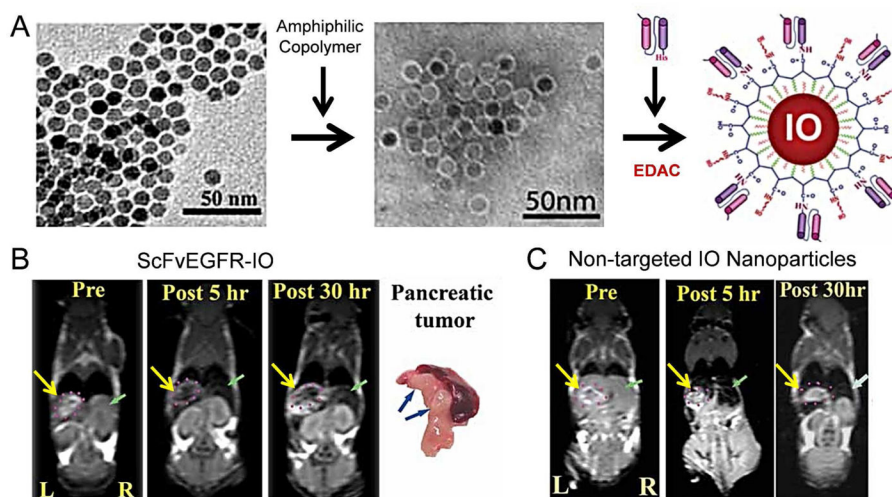


**Figure 5.** Targeting iron oxide (IO) nanoparticles with a single-chain EGFR (ScFvEGFR) antibody for MRI. **(A)** Nanoparticles were constructed by coating IO nanoparticles with an amphiphilic copolymer containing short poly(ethylene)-glycol chains. Secondly, nanoparticles were functionalized with ScFvEGFR in the presence of ethyl-3-dimethyl aminopropyl carbodiimide (EDAC). **(B)** MR images displayed enhanced pancreatic tumor contrasts (yellow arrow) in mice 5 and 30 hr post-injected with ScFvEGFR-IO nanoparticles. Also, *ex vivo* confirmation of cancerous lesions within the pancreas is shown (blue arrow). **(C)** For comparison, minimal contrasts differences are seen post-injection of non-targeted IO nanoparticles. Adapted from Ref. <sup>120</sup> with permission.

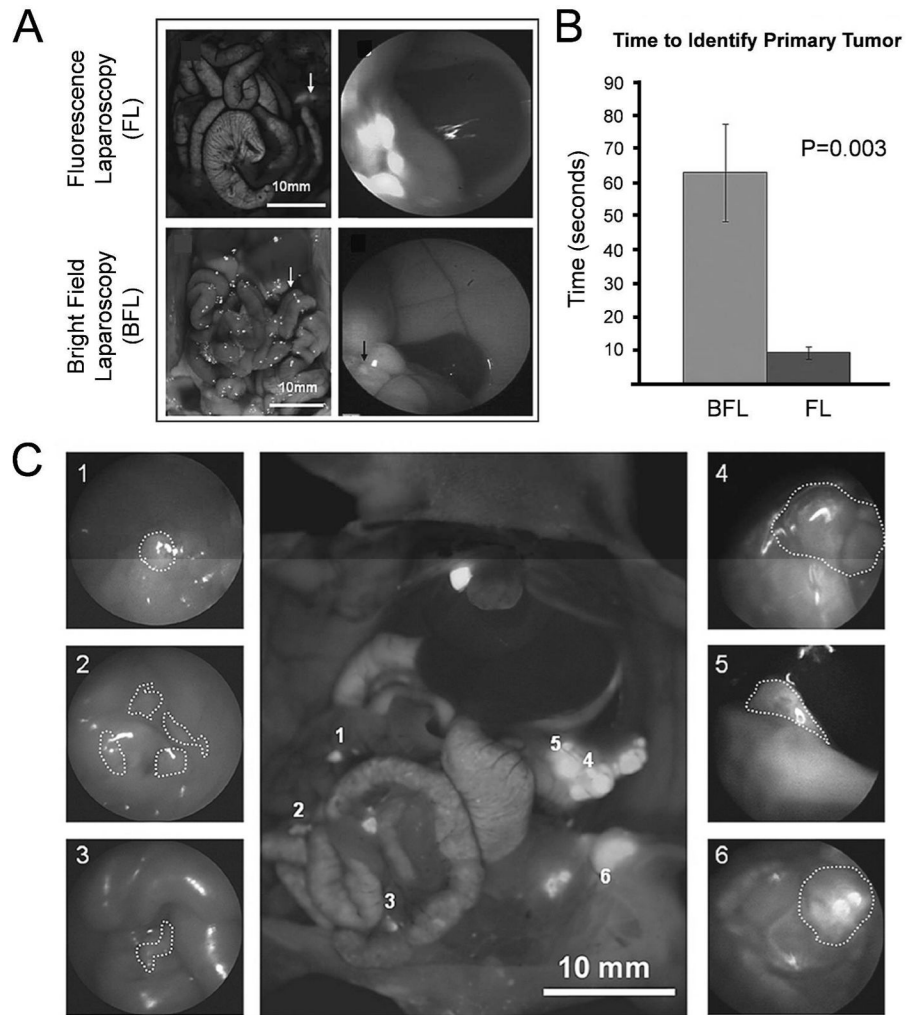


**Figure 6.** Enhanced visualization of primary and metastatic pancreatic cancer through fluorescence laparoscopy. **(A)** During laparoscopy, malignancies were easily visualized using the fluorescence mode (FL) with a fluorescent-labeled antibody. The visualization of tumors using the bright field (BFL) mode was hindered, in comparison to FL. **(B)** Time to identify the primary tumor using FL and BFL showed that FL was a much faster technique. **(C)** Using FL, both primary and metastatic lesions were easily visualized in each case. The center image represents shows six tumors in the abdomen labeled 1–6. The corresponding images of both primary tumors (4 and 5) and metastatic disease (1, 2, and 3) are shown individually. Adapted from Ref. <sup>131</sup> with permission.

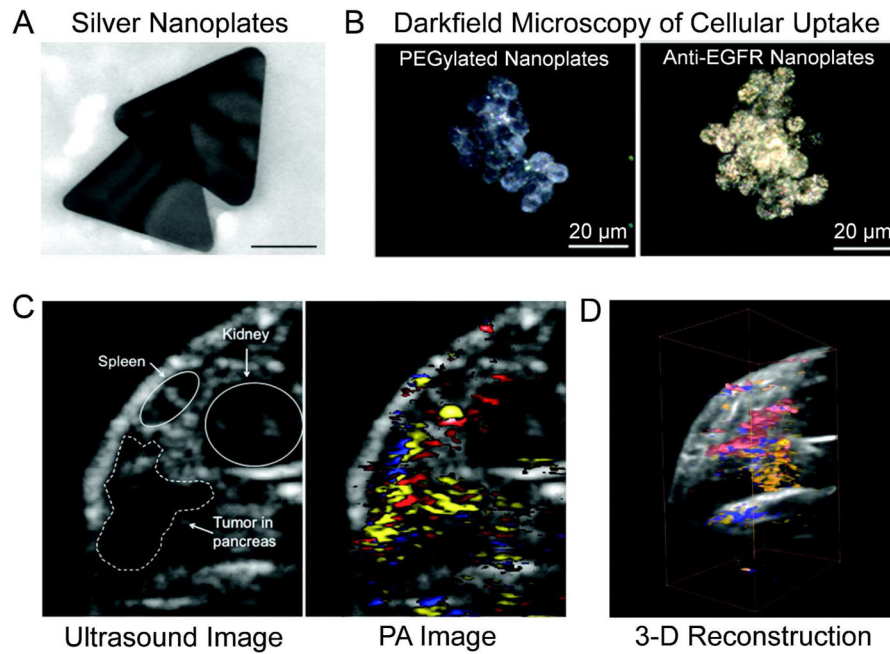


**Figure 7.** Photoacoustic imaging of pancreatic cancer using antibody-targeted silver nanoplates. **(A)** The edge lengths of silver nanoplates were  $218 \pm 35.6$  nm. **(B)** Darkfield microscopy showed increased cellular uptake of antibody-modified nanoplates (left) in comparison to PEGylated nanoplates (right). **(C)** Two-dimensional cross sections of orthotopic tumors allowed for delineation of organs and produced a photoacoustic signal from antibody-modified silver nanoplates (yellow), oxygenated blood (red) and deoxygenated blood (blue). **(D)** Image reconstruction produced a 3-dimensional representation of orthotopic pancreatic tumor model with the photoacoustic signal. Adapted from Ref. <sup>169</sup> with permission.